Carbohydrate Polymers xxx (xxxx) 118702

Contents lists available at ScienceDirect

Carbohydrate Polymers

journal homepage: www.elsevier.com/locate/carbpol

Review

Chitin and derivative chitosan-based structures — Preparation strategies aided by deep eutectic solvents: A review

Mohammad Khajavian [a], Vahid Vatanpour [b,*], Roberto Castro-Muñoz [c,d], Grzegorz Boczkaj [c,e]

[a] Department of Chemical Engineering, Faculty of Engineering, Arak University, Arak 38156-8-8349, Iran
[b] Department of Applied Chemistry, Faculty of Chemistry, Kharazmi University, P.O. Box 15719-14911, Tehran, Iran
[c] Department of Process Engineering and Chemical Technology, Faculty of Chemistry, Gdańsk University of Technology, Gdańsk 80-233, Poland
[d] Tecnologico de Monterrey, Campus Toluca, Avenida Eduardo Monroy, Cárdenas 2000 San Antonio Buenavista, 50110 Toluca de Lerdo, Mexico
[e] EcoTech Center, Gdańsk University of Technology, Gdańsk 80-233, Poland

ARTICLE INFO

Keywords:
Chitin
Chitosan
Deep eutectic solvents
Production process
Chemistry and morphology
Green chemistry

ABSTRACT

The high molecular weight of chitin, as a biopolymer, challenges its extraction due to its insolubility in the solvents. Also, chitosan, as the *N*-deacetylated form of chitin, can be employed as a primary material for different industries. The low mechanical stability and poor plasticity of chitosan films, as a result of incompatible interaction between chitosan and the used solvent, have limited its industrialization. Deep eutectic solvents (DESs), as novel solvents, can solve the extraction difficulties of chitin, and the low mechanical stability and weak plasticity of chitosan films. Also, DESs can be considered for the different chitosan and chitin productions, including chitin nanocrystal and nanofiber, *N*,*N*,*N*-trimethyl-chitosan, chitosan-based imprinted structures, and DES-chitosan-based beads and monoliths. This review aims to focus on the preparation and characterization (chemistry and morphology) of DES-chitin-based and DES-chitosan-based structures to understand the influence of the incorporation of DESs into the chitin and chitosan structure.

1. Introduction

Chitin stands out as the central constituent in a wide variety of living organisms. It can be extracted from various species including invertebrates, crustacean shells, insect cuticles, cell walls of fungi, green algae, yeast (Alishahi & Aïder, 2012), to mention just a few. After cellulose, chitin, which is a linear polysaccharide, has been announced as the second most abundant biopolymer comprising *N*-acetyl-2-amino-2-deoxy-D-glucopyranose and 2-amino 2-deoxy-D-glucose in pyranose form that are connected by 1–4 glycosidic bonds (Díaz-Montes and Castro-Muñoz, 2021a, b; Khayrova, Lopatin, & Varlamov, 2021). Chitin frequently exists in the form of nano-organized chitin-proteins, chitin-pigments, or chitin-mineral composite biomaterials in nature. Research has been focused on the exploration of chitin in medicine, biotechnology, and biomimetics (Tsurkan et al., 2021). The industrialization of chitin needs to find progressive extraction methods to standardize its utilization in the industry considering cost-effectiveness and biocompatibility. The extraction of chitin follows several steps such as demineralization, deproteinization, and deodorization. For instance, demineralization and deproteinization are the main processes that have been employed in both the chemical and biological isolation of chitin. In the chemical isolation method, minerals and proteins can be eliminated from the structure of chitin by using strong acid and alkali, respectively, resulting in a huge amount of destructive acidic or basic wastewater and severe ecological glitches. While biological methods can be performed to overcome the disadvantages of the chemical isolation process. The biological methods can be divided into enzymatic reactions and microbial fermentation. The chitin produced by the biological method owns a higher molecular weight and crystallinity, comparing to the chemical method (Hajji, Ghorbel-Bellaaj, Younes, Jellouli, & Nasri, 2015). Nevertheless, longer fermentation cycles and expensive enzymes are referenced as the main bottlenecks of the biological process (Kadokawa, Setoguchi, & Yamamoto, 2013). Interestingly, ionic liquids (ILs) are organic salts in the liquid state at room temperature (or close) that can outperform the disadvantages of chemical and biological-based methods for the efficient extraction of chitin (Yavir, Konieczna, Marcinkowski, & Kloskowski, 2020); however, recent studies disputed the green recognition of ILs because of their hazardous toxicity and very low biodegradability (Weaver, Kim, Sun, MacFarlane, & Elliott, 2010). As an alternative, deep eutectic solvents (DESs), recognized as the new green solvents, own similar features to ILs (Ul et al., 2021). However, DESs possess simpler and less expensive synthesis pro-

* Corresponding author.
E-mail address: vahidvatanpour@khu.ac.ir (V. Vatanpour).

https://doi.org/10.1016/j.carbpol.2021.118702
Received 9 August 2021; Received in revised form 21 September 2021; Accepted 21 September 2021

cedures with more biodegradability, renewability, and fewer toxicity features in comparison to ILs (Musarurwa & Tavengwa, 2021). DESs can be constructed by the connection between hydrogen bond acceptor (HBA) and donor (HBD) using H-bonding interactions to create a eutectic mixture with lower melting points compared to each constituent (Taghizadeh, Taghizadeh, Vatanpour, Ganjali, & Saeb, 2021). Fig. 1a and b displays the two most important DESs used in chitin production, which are created by the connection between HBA and HBD structures using hydrogen bonds.

DESs can be categorized into four types, such as Type I: the mixture of organic and metal salts (Makoś & Boczkaj, 2019), Type II: the mixture of organic salts and metal hydrates (Janicka, Przyjazny, & Boczkaj, 2021), Type III: combination of organic salts and specific compounds being hydrogen bond donors (Makoś, Fernandes, Przyjazny, & Boczkaj, 2018), and Type IV: combination of metal chlorides and specific compounds being hydrogen bond donors (Smith, Abbott, & Ryder, 2014). Organic synthesis, dissolution media, membrane science, extraction processes are quoted as the main application areas of DESs (Ul et al., 2021; Vatanpour, Dehqan, & Harifi-Mood, 2020). Likewise, the extraction of various biopolymers, including cellulose, lignin, starch, chitin, can be accomplished by DESs (Francisco, Van Den Bruinhorst, & Kroon, 2012). When dealing with the separation of chitin using DESs (Zhang, De Oliveira Vigier, Royer, & Jérôme, 2012), higher purified chitin was produced by employing the DESs-based method compared with other ILs-based solvents, chemical and biological techniques (Mukesh et al., 2019). Moreover, DESs can be employed to enforce the mechanical strength of chitosan structure, in principle, chitosan, as an insoluble linear natural polysaccharide, is originated from alkaline *N*-deacetylation of chitin. *N*-acetyl-D-glucosamine units connected by β-(1→4) glycosidic bonds constitute the structure of chitosan, which is a chitin-derived biopolymer with high biocompatibility, no toxicity, and excellent biodegradability (Khajavian et al., 2020a, b). Fig. 1**c** illustrates the chitin and chitosan structures. Chitosan can be generated by eliminating an acetate moiety from chitin structure using hydration (amide hydrolysis under alkaline circumstances with concentrated NaOH) or via enzymatic hydrolysis in the attendance of chitin deacetylase. The high

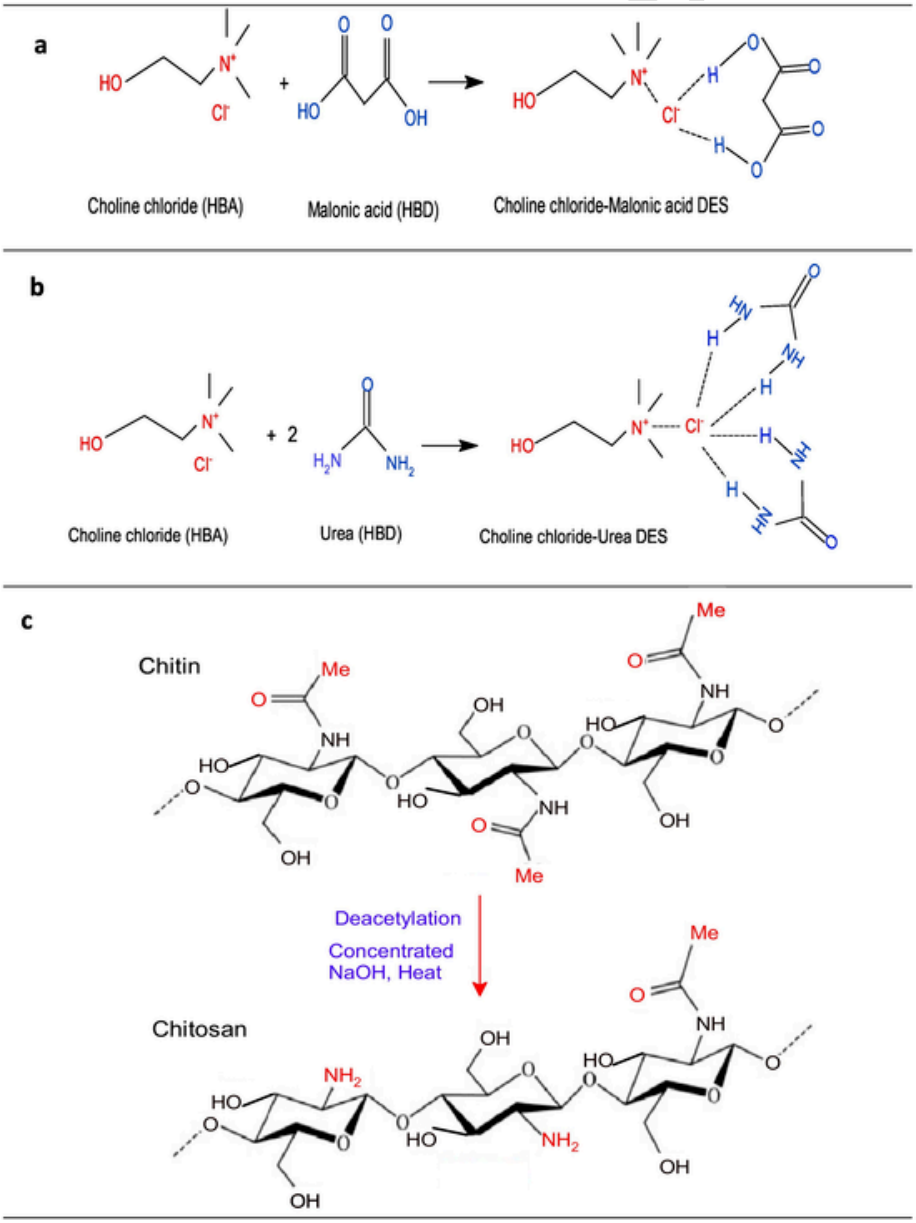

Fig. 1. The combination of HBA and HBD for DES production a) choline chloride-malonic acid DES and, b) choline chloride-urea DES), and c) chitin and chitosan structures.

functionality and outstanding film-forming properties of chitosan structure have extended the application of chitosan in various areas, including pharmacology, drug delivery, wound healing resources, biosorbents, water and wastewater treatment, and food packaging industry (Campos, Gerschenson, & Flores, 2011; Castro-Muñoz, Gonzalez-Valdez, & Ahmad, 2020; Panwar, Raghuwanshi, Srivastava, Sharma, & Pruthi, 2018). As mentioned previously, the low mechanical stability and poor plasticity of chitosan-based films restrict the industrialization of chitosan films (Naghibi, Salehi, Khajavian, Vatanpour, & Sillanpää, 2021), even if it is estimated that the worldwide chitin and chitosan market could reach $4.2 billion by 2021 from $2.0 billion in 2016 at a compound annual growth rate (CAGR) of 15.4% (Bakshi, Selvakumar, Kadirvelu, & Kumar, 2020). To date, different techniques have been utilized to raise the mechanical strength of chitosan-based films including their blending with other synthetic polymers and additives (e.g., plasticizers and surfactants) (Montalvo, López Malo, & Palou, 2012), CNTs (Salehi et al., 2013), etc. In theory, chemically-synthesized polymers can improve the mechanical stability of chitosan structure but not enough to be used in specific areas, such as membrane processes or food packaging technology. In addition to this, such a blending may reduce the biodegradability features of chitosan-based films. The utilization of DESs in the chitosan structure can noticeably upregulate the mechanical strength, plasticity, and biodegradability of chitosan films compared with synthetic polymers like polyvinyl alcohol (Mujtaba et al., 2019). The improvement of mechanical stability of chitosan films is directed to specific parameters, such as elongation at break (*Eb*), tensile strength (*TS*), and Young's modulus (*YM*). Particularly, the incorporation of DESs into the chitosan can increase the elongation at break and thus increasing the mechanical strength of chitosan films. Also, DESs are introduced as a plasticizer agent to improve the flexibility and reduce the fragility of chitosan films (Jakubowska, Gierszewska, Nowaczyk, & Olewnik-Kruszkowska, 2020). DESs can diminish the tension of deformation, hardness, density, viscosity, and the electrostatic charge of chitosan films, contributing to the high plasticity of chitosan films. Together with all these improved properties, transparency, thermal stability, the smoothness of the surface, and water vapor transmission ability can also be enhanced by using DES into the polymeric chitosan matrix (Jakubowska, Gierszewska, Nowaczyk, & Olewnik-Kruszkowska, 2021).

Very recently, Özel & Elibol (Özel & Elibol, 2021)have outlined the DES-based applications in chitin and chitosan structure, however without discussing preparation procedure, chemical properties, and morphology in detail. Understanding the preparation process is necessary to determine the most efficient and cost-effective technique to prepare DES-based chitin and chitosan structures. Also, studying the chemical properties and morphology can provide an excellent view to realize the interaction between DES and chitosan or chitin, which contribute to the better recognition of the effects of components on each other to optimize the DES-base chitin and chitosan structures.

Therefore, this review targets to analyze the current developments focused on the evaluation of the influence of DES addition on the chitin and chitosan-based structures. Particular emphasis has been made on the preparation strategies to merge the chitin and chitosan into different DES phases, discussing the most relevant findings. Also, the characterization of reported chitin and chitosan-DES forms, including chemistry, crystallinity, mechanical and thermal stability, surface morphology, were analyzed focusing on the influence of DES addition on both biopolymer structures.

2. Chitin

Chitin, as the second plentiful natural polysaccharide after cellulose, is created by *N*-acetyl-glucosamine and *N*-glucosamine (deacetylated) units distributed aimlessly and connected by β-(1–4) bond. The different orientations and packing of the chitin molecular chains result in the existence of chitin in three forms, including α-chitin, β-chitin, and γ-chitin. The α-chitin and β-chitin, owning antiparallel and parallel chains, respectively, exist naturally in crustaceans and insects, and mollusks, respectively. The γ-form of chitin has newly been mentioned as a different type of the α-chitin form but with some similarities to β-chitin. However, α-chitin includes a huge amount of hydrogen bonds, which leads to a more stable structure compared to the other two forms (Lasheen et al., 2019). The strong hydrogen bonding between the acetyl groups in the fully acetylated chitin structure limits the dissolution of chitin in the water and most organic solvents, as a result of the crystalline structure of chitin (Wang et al., 2020). Co-solvents revealed to own high capability to produce high-quality chitin from the natural environment and crustaceans (Hong et al., 2019). The dissolution and extraction of chitin by DES solvent have shown to be superior methods in comparison to other solvents considering straightforwardness, effectiveness, and biocompatibility. The high selectivity of DES structure towards chitin contributes to obtaining it with high purity. Furthermore, DESs are considered as the solvent to convert chitin powder into chitin nanocrystals and nanofibers, which are more effective as a result of high surface area and crystallinity for a wide range of utilization like adsorption.

2.1. Chitin production techniques using DESs

Acid hydrolysis with a strong acid and the subsequent mechanical fragmentation of products is cited as the typical technique to produce chitin nanocrystals. TEMPO (2,2,6,6-tetramethylpiperidine-1-oxyl radical oxidation)-mediated oxidation of α-chitin and the following ultrasonic process can be employed to generate chitin nanocrystals with high crystallinity. In the TEMPO process, the hydroxyl groups of chitin are oxidized to own higher density compared to carboxylate groups (Fan, Saito, & Isogai, 2008). To avoid the oxidation of the chitin surface, a hydrochloric acid hydrolysis technique can be performed on the chitin structure for 60–120 min, then diluted by distilled water (Tan, Lee, & Chen, 2020). The hydrolysis process is unrecyclable with large produced acidic waste. DESs, as a new method for chitin production, outperform in the production of chitin contrasted to conventional methods, as a result of higher biocompatibility, biodegradability, and cost-affectivity. Likewise, reusability of DESs, adjustability of acidity of DESs solutions by changing the molar ratio between HBA and HBD, and the selectivity of DESs towards pure chitin structure in the dissolution process, can be influential in the chitin extraction process, and chitin production in the different forms including nanocrystals and nanofibers (Ramírez-Wong et al., 2016). The superiority of the raw material and solvent, along with the efficiency of the practical processes and the features of the water, influence the quality of prepared chitin. Inappropriately, the necessity of storing raw materials for a long time can affect the quality of raw materials, causing a reduction in chitin quality (Huet et al., 2020). This practical procedure can be changed to improve the dissolution and functionality properties of chitin produced by DES. Also, proper pre-treatment and/or storage strategies of raw materials, together with the fitting of the applied procedure, can be utilized to generate chitin with high quality using DESs solvents (Trung et al., 2020). It was reported that a three-step physical pretreatment, including drying, grinding, and sieving, can eliminate the protein and ash contents from the chitin structure without reducing in chitin yield (Hamed, Özogul, & Regenstein, 2016). However, likely, these typical methodologies may not satisfy the current demand and requirements of chitin. Therefore, different strategies have been proposed to produce or modify chitin. For instance, Yuan and his colleagues utilized choline chloride (ChCl)-based DES including different acidic HBDs (e.g., oxalic acid, lactic acid, malonic acid, citric acid, and DL-malic acid) to fabricate chitin nanocrystals, as presented in Fig. 2a (Yuan, Hong, Lian, Zhang, & Liimatainen, 2020).

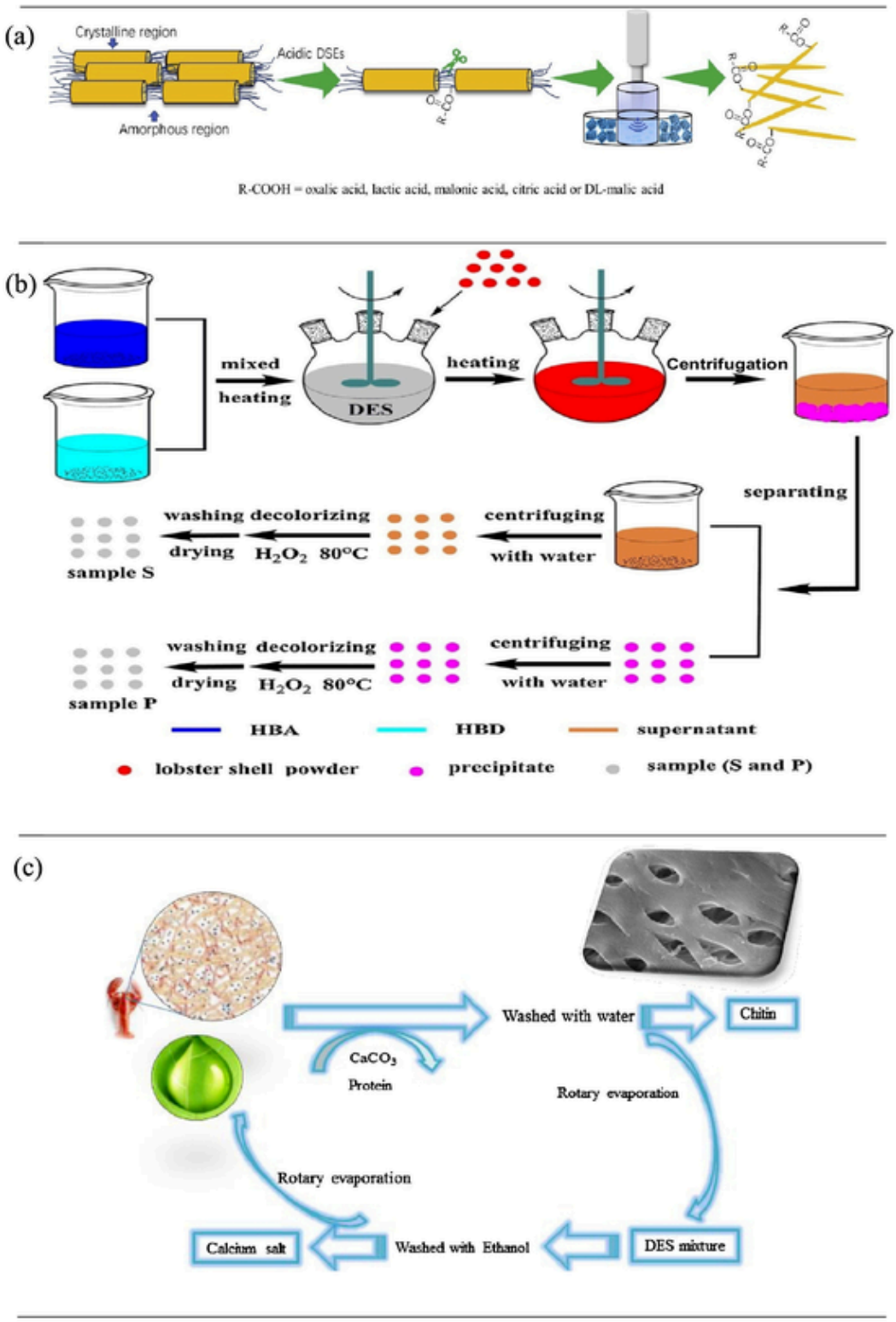

Fig. 2. a) Graphical representation of chitin nanocrystal production process using DESs (Yuan et al., 2020) (License number 5039160731302), b) graphical drawing of chitin extraction from lobster shells using DES (Zhu, Gu, Hong, & Lian, 2017) (License number 5039161449479), c) strategy used for the extraction of chitin from Lobster shell (Hong, Yuan, Yang, Zhu, & Lian, 2018) (License number 5039170306918).

In a different study, various DESs, including ChCl and betaine (acting as HBAs) and organic acids, urea and glycerol (as HBDs), were evaluated considering their effectiveness in deproteinization and demineralization for the preparation of chitin from the skimmed black soldier fly. The mixture, including the insect (5 g) and different DESs (50 g), was shaken at a temperature of 80 °C for 2 h. Chitin particles were subsequently removed by a filtration process, followed by a washing method utilizing deionized water, and finally air-dried at 80 °C in an oven (Zhou et al., 2019). As a preliminary remark, it was proved that that H^+ coming from HBA or HBD was the main agent for demineralization, while intermolecular and intramolecular hydrogen bonds in natural DESs facilitated the removal of protein (Zhou et al., 2019). Cao et

al. employed *p*-toluenesulfonic acid-ChCl (PTA-ChCl) DES to produce the chitin nanocrystals. Similar to previous reports, the optimized amount of chitin powder (5 wt%) and DES solution was stirred at 95 °C for 30 min. Then, the DES-chitin blend was centrifuged for 20 min at 4000 rpm. Afterward, ethanol was added to the centrifuged chitin to acquire a gel-like blend. This blend was then centrifuged for 20 min at 4000 rpm. The residual centrifuged chitin was washed twice by ethanol and then dried under lyophilization (Jiang et al., 2020). In a further investigation, the study explored the ability of the nanocrystals as immobilization support of porcine pancreas lipase, exhibiting good credentials in biocatalysis (Jiang et al., 2020). Chloride-based DESs (e.g., ChCl-thiourea, ChCl-urea, ChCl-glycerol, and ChCl-malonic acid) were employed to obtain chitin from lobster shells (Zhu et al., 2017), as illustrated in Fig. 2b.

Finally, since the resulting chitosan had a porous structure, it represents a promising material for adsorption (Castro-Muñoz, Gonzalez-Melgoza, & Garcia-Depraect, 2021) and tissue engineering (Pérez-Guzmán & Castro-Muñoz, 2020) applications. By using similar ChCl-thiourea DES, Mukesh and his coworkers produced the α-chitin nanofibers, where pure chitin powder (10 wt%) was poured into the DES solution, the DES-chitin blend was agitated at 500 rpm at 100 °C for 2 h. The obtained gel-like material was diluted by adding 10 mL of distilled water. The distributed chitin was centrifuged at 10,000 rpm for 10 min and then washed with deionized water to deacidify. The deacidified chitin was subsequently ultrasonicated and followed by nanofiber dehydration via lyophilization procedure (Mukesh, Mondal, Sharma, & Prasad, 2014). The final chitin material was used to synthesize calcium alginate bionanocomposite gel beads for drug delivery, which displayed improved elasticity compared with typical Ca-alginate beads.

The acidic DESs based on citric, lactic, and malic acids were utilized to produce *O*-acylated chitin from shrimp shells in simultaneous decalcification, deproteinization, and acylation processes. In this study, the molar ratio of both HBA and HBD elements forming the DES was evaluated since their molar ratio greatly defines the physicochemical properties (solubility, viscosity, etc.) of the resulting eutectic mixture (Sarmad, Xie, Mikkola, & Ji, 2016). Similar to Yuan's study (Zhou et al., 2019), Feng et al. also stated that H^+ release from ChCl–DL malic acid was the main responsible to remove calcium carbonate and start acylation reaction. Here, the protein was decomposed into amino acids thanks to the acidity of the DES and hydrogen bonding formation (Feng et al., 2019).

Lobster shell powder was also treated with four different ChCl-based DESs (Hong et al., 2018). The overall production process is represented in Fig. 2c (Hong et al., 2018). The ability of deproteinization and depolymerization of DES was associated with the acid used. The ChCl-malonic acid offered the highest yield (~22%) and purity (~93%). It is worth mentioning that the kind of used DES, depending on the type of organic acid and temperature, influenced the molecular weight of the resulting chitin. Moreover, after the morphological characterization, it was noted that the resulting chitin owned a width ranging from 400 to 1000 nm, while the chitin fibers showed an arrangement side by side. Also, chitin displayed a porous structure, which opens the possibility to use it for targeted applications, e.g., adsorption of dye and metal ions (Ursino et al., 2018).

Ramirez-Wong and his colleagues proposed ChCl-urea and hexafluoroisopropanol (HFIP) to tune the crystallization of chitin-based films with β-dihydrated- or γ-chitin structures (Ramírez-Wong et al., 2016). A ChCl-urea with a molar ratio of 1:2 was combined with chitin (2 wt%) from shrimp shells, which were later agitated at 100 °C to attain a homogeneous solution. To some extent, the interaction of α-chitin with ChCl-urea fostered a γ-mono-phase in the films, which is illustrated in Fig. 3 (Ramírez-Wong et al., 2016).

Zhao and his colleagues eliminated minerals and proteins from shrimp shells to produce chitin powder. Deproteinization and demineralization processes were performed by different DESs (betaine HCl-urea, ChCl-urea, ChCl-ethylene glycol, ChCl-glycerol) with the assistance of microwave, and citric acids, respectively (Zhao, Zhu, et al., 2019). In another study, shrimp shells and DESs were mixed with the different ratios of 1:5, 1:10, and 1:20, then the mixture was heated (700 W microwave irradiation) and centrifuged to remove chitin powder (Huang, Zhao, Guo, Xue, & Mao, 2018).

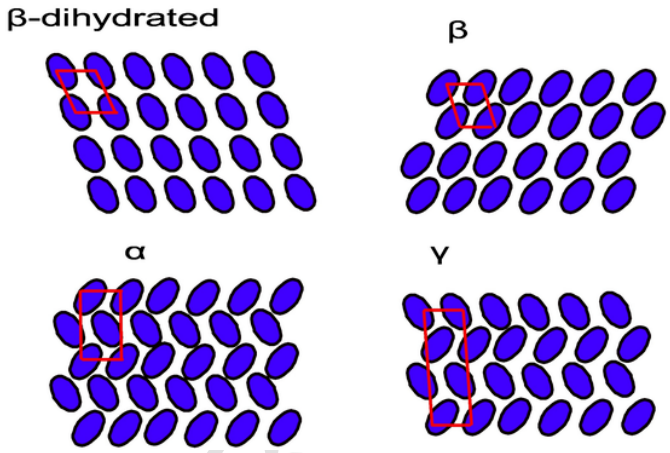

Fig. 3. Illustration of chitin chain arrangement in the phases β-dihydrated, β, α, and γ.

Commonly, the extraction process of chitin can be started by the dissolution of raw chitin resources into the DES solution, which causes the DES-chitin solution, in which chitin structure is dissolved in the DES, and the minerals and other components stay undissolved. Then, the minerals are removed from DES-chitin solutions by centrifugation process. Pure DES-chitin is processed in a water coagulation bath, to revitalize (or to 'crystallize') the polymer and remove the DES. The crystallized chitin polymer is furthermore rinsed by deionized water to remove DES. The combination of raw material of chitin with chloride-based DES at 100 °C for 2 h can be proposed for production or modification of chitin structure. In addition, microwave and ultrasonication processes can cause time and temperature reduction necessary for chitin dissolution. While the hot glycerol trailed by grinding in the citric acid could remove impurities from the chitin structure. The utilization of hot water and CO_2 can result in chitin with a high degree of purity (~90%) (Van Hoa, Vuong, Minh, Cuong, & Trung, 2020). Table 1 compares the degree of deacetylation and the yield of different produced chitins considering different sources of chitin and DES. The combination of betaine hydrochloride (HBA)-ferric chloride hexahydrate (HBD) DES and shrimp shell, as the resource of chitin, showed the highest yield for the production of chitin nanocrystals, in comparison to other conditions. Also, the degree of deacetylation was recorded as high as 95.59% for the mixture of betaine-urea DES and chitin originated from insects. In the next sections, the chemistry and morphology of the resulting DES-chitin structures will be discussed meticulously.

Generally, shellfish wastes include proteins, lipids, minerals, pigments, and chitin. The most efficient method for chitin extraction can isolate the most amount of chitin and remove the other ingredients as much as possible. The demineralization process using DES, as the first step in chitin extraction, is the most important part. The HBA of DES is the determining factor for high chitin extraction from raw material. The more efficient HBA can remove more minerals from the spaces between the chitin-protein fibers which leads to the better deteriorating of the connection within the inner structure of shellfish waste and a better dissolution process. Also, the second step is deproteinization of demineralized chitin, which can be affected by the strength of DES to disrupt the hydrogen bond of the demineralized shellfish waste structure. The better-demineralized waste means the higher penetration of DES into the

Table 1
Yield and degree of deacetylation comparison for variously produced chitins from different sources and DES combinations.

The source of chitin	HBA	HBD	Application	Yield (%)	Degree of deacetylation (%)	Ref.
Crab shell	ChCl	Oxalic acid dihydrate	Chitin nanocrystals production	79.5	–	(Yuan et al., 2020)
Crab shell	ChCl	Lactic acid	Chitin nanocrystals production	87.5	–	(Yuan et al., 2020)
Crab shell	ChCl	Malonic acid	Chitin nanocrystals production	84.1	–	(Yuan et al., 2020)
Crab shell	ChCl	Citric acid monohydrate	Chitin nanocrystals production	82.3	–	(Yuan et al., 2020)
Crab shell	ChCl	DL-Malic acid	Chitin nanocrystals production	79.6	–	(Yuan et al., 2020)
Insect chitin (*Hermetiaillucens*)	Betaine	Urea	Chitin extraction (powder)	26.71	95.59	(Zhou et al., 2019)
Insect chitin (*Hermetiaillucens*)	Betaine	Glycerol	Chitin extraction (powder)	25.47	89.52	(Zhou et al., 2019)
Insect chitin (*Hermetiaillucens*)	Betaine	DL-lactic acid	Chitin extraction (powder)	25.70	88.29	(Zhou et al., 2019)
Insect chitin (*Hermetiaillucens*)	Betaine	Oxalic acid	Chitin extraction (powder)	22.85	84.17	(Zhou et al., 2019)
Insect chitin (*Hermetiaillucens*)	Betaine	n-Butyric acid	Chitin extraction (powder)	24.53	94.39	(Zhou et al., 2019)
Insect chitin (*Hermetiaillucens*)	ChCl	Urea	Chitin extraction (powder)	22.82	80.19	(Zhou et al., 2019)
Insect chitin (*Hermetiaillucens*)	ChCl	Glycerol	Chitin extraction (powder)	22.85	91.48	(Zhou et al., 2019)
Insect chitin (*Hermetiaillucens*)	ChCl	DL-lactic acid	Chitin extraction (powder)	16.4	70.34	(Zhou et al., 2019)
Insect chitin (*Hermetiaillucens*)	ChCl	Oxalic acid	Chitin extraction (powder)	23.25	90.70	(Zhou et al., 2019)
Lobster shell	ChCl	Malic acid	Chitin extraction (Powder)	90	95.11	(Hong et al., 2018)
Shrimp shells	ChCl	Malic acid	O-acylated chitin production	56.60	–	(Feng et al., 2019)
Commercial chitin	ChCl	Thiourea	Nanofiber production	84	–	(Feng et al., 2019)
Lobster shells	ChCl	Malonic acid	Chitin extraction (Powder)	20.36	–	(Zhu et al., 2017)
Shrimp shells (*Marsupenaeus japonicas*)	ChCl	Malonic acid	Chitin extraction (Powder)	19.41	–	(Saravana et al., 2018)
Shrimp shells	Betaine hydrochloride	Ferric chloride hexahydrate	Chitin nanocrystals production	88.5	–	(Hong, Yuan, Zhang, Lian, & Liimatainen, 2020)
Shrimp shells	ChCl	$ZnCl_2$	Chitin nanocrystals production	61.6	–	(Hong et al., 2019)
Shrimp shell	Betaine HCl	Urea	Chitin powder	23	–	(Zhao, Huang, et al., 2019)
Shrimp shell	ChCl	Urea	Chitin powder	25	–	(Zhao, Huang, et al., 2019)
Shrimp shell	ChCl	Ethylene glycol	Chitin powder	24	–	(Zhao, Huang, et al., 2019)
Shrimp shell	ChCl	Glycerol	Chitin powder	22	–	(Zhao, Huang, et al., 2019)
Shrimp shell	ChCl	Malic acid	Chitin powder	More than 80	–	(Huang et al., 2018)
Shrimp shell	ChCl	Malic acid	Chitin powder	–	33	(Vicente, Huš, Likozar, & Novak, 2021)
Shrimp shell	ChCl	Oxalic acid	Chitin powder	–	20	(Vicente et al., 2021)

inner structure of waste material and more disruption of hydrogen bond consequently improved chitin deproteinization and extraction.

2.2. Characterization of DES-chitin structures

The different combinations between DES and chitin, the resources of raw chitin, together with the preparation methods, can influence the character and chemistry of produced DES-chitin structure. It is essential to study the chemistry and morphology of prepared DES-chitin structures to understand the chemical interaction between different components in the DES-chitin network and, the effect of these interactions on the morphology of formed DES-chitin. Therefore, the chemistry, including the interaction between different functional groups of DES and chitin structures, will be detailed in the next section. Also, the morphology, containing crystallinity, surface morphology, and the mechanical and thermal stability of prepared DES-chitin constructions have been detailed.

2.2.1. Chemical properties of DES-based chitin structures

The hydroxyl (OH) groups of chitin are substituted by the acetyl amine group, which contribute to a poly (*N*-acetyl D-glucosamine) or poly-β-[1,4]-*N*-acetyl-D-glucosamine structure of chitin. The degree of acetylation (DA) and deacetylation (DD), as important parameters of prepared chitin, can be defined by the repetitive units of *N*-acetylated β-1,4-D-glucosamine in the biopolymer and the percentage of β-1,4-D-glucosamine units in the polysaccharide, respectively (Joseph, Krishnamoorthy, Paranthaman, Moses, & Anandharamakrishnan, 2021). The area of chitin application can be assigned by the viscosity and molecular weight of chitin. For instance, chitin with low and high molecular weight can be employed in environmental (high biodegradability) and tissue engineering (high strength), respectively. Also, the chitin with high DA is more suitable for nutraceutical delivery systems as a result of gentler degradation rates to lysozymes. The α-chitin arrangement can be found in the abundant sources, including krill, lobster, crab, and insect. Delipidation, demineralization and, deproteinization of chitin by chemical materials are traditional steps to extract

chitin from raw materials. 80% of fats in the triacylglycerol form in chitin can be removed by using ethanol at high temperatures that results in eliminating useful materials such as organic aromatic compounds in the duration of delipidation. The splitting chemical bonds between chitin and proteins in the deproteinization process need a long time, which causes an expensive chitin extraction process. Additionally, calcium carbonate and different acids, including sulfuric, hydrochloric, and nitric, are involved to extract chitin from the raw sources in demineralization. In this technique, the breakdown of calcium carbonate into calcium chloride emits carbon dioxide. Chemically hazardous materials and unsafe processes have been announced for the demineralization process (Mohan et al., 2020). In addition, low crystallinity, and prolonged hydrogen bonding resulted in the low solubility and reactivity of chitin produced by traditional methods, restrict the industrialization and commercialization of chitin (Pădureţu, Apetroaei, Rău, & Schroder, 2018). DESs can be utilized to practicalize the employment of chitin in the industry by enhancing the solubility of chitin, and the straightforwardness and biodegradability of the chitin extraction process. The straightforward synthesis procedure, non-toxicity, reusability and, biodegradability are cited as the main superior features of DES solvents contrasted to other conventional solvents (Kumar et al., 2020). DESs are widely consumed in biomass processing such as chitin extraction since they have negligible volatility and are water-miscible at room temperature. From the chemistry point of view, the disruption of the hydrogen bonding network is essential to dissolve chitin in the DES solution. The polarity of DES and β-chitin value, as well as the kind of HBA and HBD in the DES, can affect the solubility and extraction process of chitin. The three forms of chitin (α-, β-, and γ-chitin) own a strong hydrogen bonding network using the hydroxyl and *N*-acetyl groups in the chitin structure (–NH···O═C and –OH···O═C hydrogen bonds). The parallel structure of *β*-chitin and antiparallel structure of α-chitin contribute to the intra-polymer interactions. The more effective selection of DES means the more influential chitin extraction process. The more selective dissolution of chitin with higher disruption of hydrogen bonding can cause a more effective extracted chitin process by DES solvent. The structure of DES comprises a cation, an anion, and a neutral constituent. For instance, the anions of DES solvent can perform the dissolution process of chitin from raw biomaterial such as shrimp shells. In DES, the cations belonging to the HBD's of DES solvent bind to the anions of HBA, which cause a complex bulky ion. Then, anions create a hydrogen bond with the proton from the OH group in the chitin. Consequently, the cations of HBD in the DES simply interact with the corresponding anions in the shrimp shell structure (Zulkefli, Abdulmalek, & Abdul Rahman, 2017). Many other operational factors can influence the interaction between chitin and DES. The molar ratio between HBD and HBA, temperature, and pH of DES mixture, along with the raw material of chitin, can influence the quality of produced chitin structure. Studying the chemistry of DES-chitin networks, e.g., using analysis like FTIR can present valuable information regarding DES and chitin interactions.

The mixtures of ChCl (HBA) and various organic acids (HBD), including oxalic acid, lactic acid, malonic acid, citric acid, and DL-malic acid, have been evaluated in the construction process of chitosan nanocrystals originated from crab shells. DES, containing lactic acid, malonic acid, and citric acid, displayed higher differences in particle size distribution and higher transparent chitosan nanocrystals in comparison to oxalic acid and DL-malic acid, as a result of the reaction between carboxylic acids of DES and hydroxyl groups of chitin, which caused ester bonds. Ester groups play as a steric wall that chunks hydrogen bonding between the chitin chains, which contribute to improving chitin disintegration to produce nanocrystals. DES-based chitin nanocrystals exhibited outstanding dispersibility in water, which is valuable in producing composites covering dispersed chitin-based structures for water treatment utilization. The mass yield of chitin nanocrystals generated by DES showed a superior amount compared to traditional mineral acid hydrolysis-based chitins because of the esterification process of the hydroxyl groups of chitin established from the creation of monoester or diesters. Differently from pure chitin, FTIR analysis revealed the connection between carbonyl vibrations of ester and carboxylic acid group (1734 cm^{-1}) in the DES-based chitin (Yuan et al., 2020).

Different DESs were synthesized by the combination of ChCl and betaine, as HBAs, and organic acids (oxalic acid, lactic acid, and butyric acid), urea and glycerol, as HBDs. The degree of the acidity of the HBD was reported as oxalic acid > lactic acid > butyric acid > glycerinum > urea. The result showed that when ChCl (HBA), as an alkali chemical, mixed with an HBD with lower pH can produce chitin with higher yield and a higher degree of deacetylation (DD) values. Equally, the combination of betaine (HBA) as an acidic chemical and an HBD with more pH value can result in chitin with more DD (Zhou et al., 2019). The existence of amide I band (1624 and 1660 cm^{-1}) proved the creation of two kinds of hydrogen bonds between carbonyl groups of DES, and –NH and –OH groups of chitin. The functional groups of raw chitin remain unchanged in the conversion process of chitin to nanocrystals using *P*-toluenesulfonic acid/ChCl DES (Jiang et al., 2020). ChCl-thiourea DES-based chitin displayed higher purity in contrast to other DES-based chitin (ChCl-urea, ChCl-glycerol, and ChCl-malonic acid). The amide band was identified by 1477 cm^{-1} in the FTIR analysis, which was stronger for ChCl-thiourea DES-based chitin compared with other DES-based chitins. The more existence of amide bands in the chitin structure means the higher removal of proteins from the chitin structure, which causes purer chitin (Zhu et al., 2017). The FTIR results of the ChCl-thiourea DES-chitin structure demonstrated the presence of DES-extracted chitin in calcium alginate beads, which can be consumed in the pharmaceutical industry for drug delivery (Mukesh et al., 2014). The eutectic mixture of ChCl and organic acids, including L-lactic acid, L-malic acid, D-malic acid, DL-malic acid, and citric acid, was used to carry out the decalcification and deproteinization of raw chitin towards O-acylated chitin production. Following the FTIR analysis, the amide I peak, as a sign of protein, disappeared in the DES-based chitin compared with the pristine chitin. The production of O-acylated chitin was approved by the additional bands (1738 cm^{-1}) related to the C═O group in the FTIR analysis of DES-based chitin. DES showed the impressive ability to simultaneously eliminate the calcium carbonate and protein from the chitin structure, which led to purer chitin. The protein and calcium carbonate removal was influenced by the components and the mole ratio of the organic acid in DES, and the pH of DES solutions, respectively. L-Malic acid-produced chitin exhibited higher protein removal as a result of the higher acidity of the DES solution. L-Malic acid was selected as the optimal HBD to evaluate its effectiveness on the degree of acylation of chitin. The effect of operational conditions was evaluated in producing chitin. The temperature (~130 °C) was recorded as the optimal temperature to fabricate chitin with the highest yield. The higher temperature demonstrated the more beneficial in removing carbonate and protein from the chitin structure. The influence of the mole ratio between shrimp shells and DES was examined. The outcomes showed that the increased amount of DES in comparison to shrimp shells can destroy the hydrogen bonding network of the amino group and thus decrease the yield of produced chitin. The molar ratio of 1:10 between shrimp shells and malic acid was announced as the optimal molar ratio (Feng et al., 2019). Dissolution of chitin contains two main steps including demineralization and deproteinization. The space between the chitin-protein fibers is occupied with proteins and minerals. The superiority of demineralization depends on the ability of HBA to remove minerals (crystalline $CaCO_3$) from the spaces between the chitin-protein fibers which causes the failure of the linkages within the inner structural organization of the shrimp shells and superior dissolution process. Also, the extent of chitin deproteinization depends on the amount of hydrogens bonds formed between DES and shrimp shell components. The hydrogen bond interactions in the shrimp shells are debili-

tated by contending hydrogen bond formation between the DES structure and carbohydrates of shrimp shells structure, which contribute to the breakage of the intramolecular hydrogen bond network of shrimp shell, chitin dissolution in DES, and chitin separation from the proteins. Lobster shell samples were preliminarily demineralized by a hydrochloric acid-pre-treated process. The deproteinization of the lobster shell was performed using ChCl-based DES mixtures. At this point, the DESs were prepared by merging ChCl and different HBD (e.g., malonic acid, malic acid, lactic acid, levulinic acid). The order of magnitude of deproteinization of lobster shell samples was attributed to the kind of acid used in HBD, as follows: ChCl-malonic acid > ChCl-Lactic acid > ChCl-malic acid > ChCl-levulinic acid. The partial hydrolysis of chitin under a high concentration of acid condition of DES led to lowered viscosity of DES-treated chitin compared to chitin extracted by conventional methods. Moreover, glycosidic bonds in chitin were hydrolyzed by the acidity of DES mixtures causing a reduction in molecular weight.

The DA of chitin was recently evaluated using different DES mixtures. The outcomes revealed that the different DESs own minimal influence on the DA of chitin. As shown in FTIR analysis, it was proved that the chemistry of DES-treated chitin and pure chitin is almost identical. O—H and N—H stretching, CH_2 asymmetric stretching, CH, CH_3 symmetric stretching, and three significant amide bands (Amide I, Amide II, and Amide III) appeared in both DES-extracted chitin and chitin. However, the disappearance of the 1477 cm^{-1} band in DES-extracted chitin compared to pure chitin was ascribed to the deproteinization effect of DES (Hong et al., 2018). In a different work, ChCl-lactic acid and betaine-glycerol increased the disruption of chitin's robust hydrogen bonding and facilitated the NaOH penetration compared to ChCl: oxalic acid, which caused higher deacetylation and dissolution. The high degree of deacetylation (ca. 80%) for chitin produced by DES was comparable with other conventional methods for chitin extraction (Vicente, Bradić, Novak, & Likozar, 2020).

Many reasons can be mentioned for the appropriateness of DESs as solvents for the extraction, and production of chitin in different forms, including powder, nanocrystals, and nanofibers. The donating and accepting capability of protons and electrons in the DES structure affect the efficiency of the chitin extraction process, which can increase or decrease the attendance of hydrogen bonding, and consequently, increase or decrease the dissolution ability of DES. The more NH_2 or OH groups in DES structure and a robust intermolecular hydrogen bonding reduces the ability of DES for the collapse and dissolution of chitin. Existing of strong electron-withdrawing groups in DESs accelerates the disruption of hydrogen bonds, therefore increase the dissolution of the chitin. Fig. 4 displays the general dissolution process of chitin, where the acetamido and hydroxyl groups of the chitin structure were concentrated by HBA molecules of DES solutions, resulting in the cleavage of intra- and intermolecular hydrogen bonds of chitin (Fig. 4a).

Then, HBAs were connected to chitin (NH–HBA–HO) by hydrogen bonding, which contributed to the twisting and peeling of the molecular chain. Instantaneously, HBD molecules of DES penetrated gaps between the molecular chains and thus prohibited restoration of the crystalline phase of chitin after the peeling (Fig. 4b). Lastly, the chitin chains were distributed in solution as the entirely isolated molecular form (Fig. 4c). The stable and crystalline features of chitin limit the processability and solubility of raw chitin. In addition, the existence of acetamido groups, which contribute to the preservation of intra- and inter-molecular hydrogen bonds, can increase the toughness of the chitin structure to be dissolved. The anions of DES solvents tie to acetamido and hydroxy groups of chitin chain using hydrogen bonds which give rise to deteriorating both the intra- and intermolecular hydrogen bonds (NH…O═C and OH…O═C) in the crystalline structure of chitin, and flexibilization of chitin chain. Also, the interaction between functional groups of DES, such as chlorides, and acetamido and hydroxyl groups of chitin, leads to a reduction in the solubility of chitin in the DES solvents (Sharma, Mukesh, Mondal, & Prasad, 2013).

Furthermore, the high acidity of DES solution can raise hydrogen bonding disruption of chitin structure, and increase chitin dissolution process out of consideration of the subtle nature of chitin when unprotected from acids. The higher temperature of the DES-chitin mixture can contribute to the more collapse of connections between the intermolecular hydrogen bonding of chitin, and easier the dissolution of chitin structure. From the biocompatibility point of view, most of the DESs are based on simple components, such as organic acids (lactic, malic, citric, succinic acids) and primary metabolites (such as amino acids and choline), which exist in the living cells conferring high biocompatibility.

2.2.2. Morphology of DES-based chitin structures

The surface morphology of chitin can be divided into five different categories, comprising 1) rough and hard surface morphology without any nanofibers and pores, 2) only nanofibers, 3) the combination of pores and nanofibers, 4) two types of pores in combination with nanofibers, and 5) only pores (Li, Qin, & Zhao, 2020). As previously mentioned, higher porosity and crystallinity of chitin structure mean more usability of chitin in heavy metal removal with higher adsorption capacity (Duan et al., 2013). Moreover, chitin with fibrillar surface construction can be beneficial in the textile industry. For example, the α-form, as the dominant form of chitin compared to β- and γ-forms with anti-parallel packing, owns the layers of approximately 20 single chains, in which the fibrils are steadied by the intramolecular interaction between hydrogen bonding (Liao & Huang, 2020). The number of hydrogen-bonding interactions in the chitin structure determines its thermal and mechanical stability. The more hydrogen bonding between chitin structure and water molecules in the extraction process means less intramolecular interactions between hydrogen bonding of chitin network with lower packing tightness and strength, which cause chitin with lower crystallinity, and mechanical and thermal stability (Q. Ma et al., 2020). In addition, the high degree of hydration or acidic hydrolysis of chitin can decrease the thermal and mechanical stability because of a reduction in the numbers of inter-and intra-molecular hydrogen bonding (Singh, 2019). Crucially, the appropriate selection of solvent for chitin extraction to prevent a reduction in the mechanical and thermal stability, and crystallinity, is the main challenge in chitin production, which in fact can be solved by DESs. Chitin extraction using DESs has been focused to raise the crystallinity, thermal stability, mechanical strength, and cost-effectivity of produced chitin. DES can be utilized in chitin extraction without disrupting inter-and intra-molecular hydrogen bonding in the chitin structure. SEM analysis can be employed to comprehend the surface morphologies of the chitin produced by DES, while other features of the chitin, such as physical, mechanical, and crystallinity stability, can be evaluated by XRD analysis. Also, TG analysis is a reliable method to estimate the thermostability of chitin. Thermal stability can indeed decide the possibility of chitin usage in the applications such as extreme biomimetics.

Chitin nanocrystals, created from crab shells, were prepared by the DES solvent originated from mixing ChCl and various organic acids, including oxalic acid, lactic acid, malonic acid, citric acid, and DL-malic acid. AFM analysis recorded sizes from 29 to 83 nm for the diameter of chitin nanocrystals. Furthermore, the length of malonic acid-based chitin nanocrystals displayed the shortest quantity among other DES-based nanocrystals chitins, which was attributed to the easy penetration of malonic acid into the amorphous part of chitin, enhancing the hydrolysis process. High compatibility between DESs and chitin structures preserved the crystallinity of DES-base chitin nanocrystals contrasted with pristine chitin structure. Lactic and DL-malic acid DES-based chitin nanocrystals proved lower thermal stability compared to pure chitin, while oxalic acid, malonic acid, citric acid-based DES chitin nanocrystals showed unchanged thermal stability. The stability of

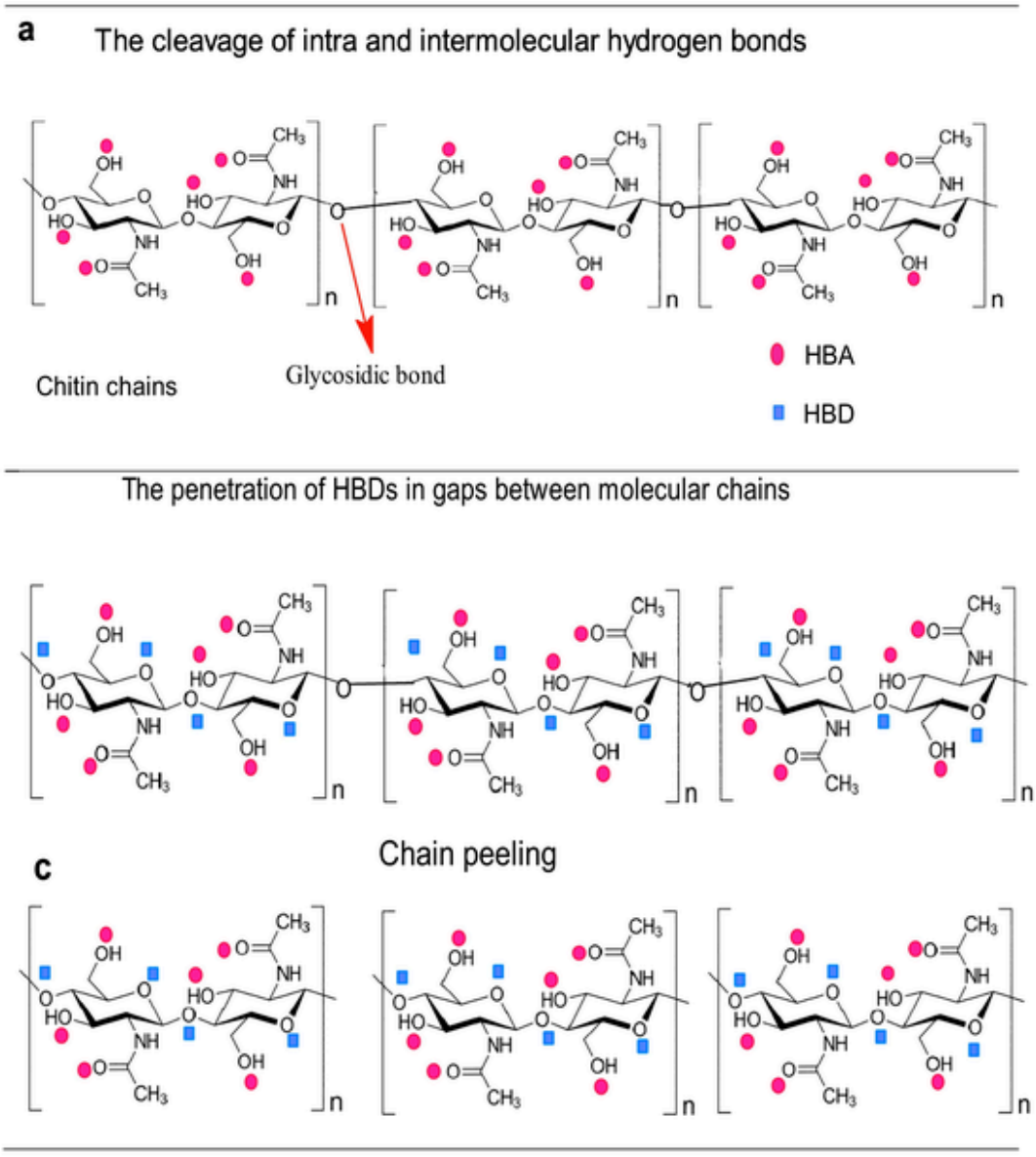

Fig. 4. Dissolution process of chitin by DES made of hydrogen bond acceptor (HBA) and hydrogen bond donor (HBD).

chitin nanocrystals at high temperature for chitin processing (up to 200 °C) demonstrated themselves as potential reinforcements for hydrolysis.

DESs can decrease or increase the crystallinity of chitin. The breaking of intramolecular and intermolecular hydrogen bonds and the formation of amorphous chitin, as a result of DES utilization, can decrease the crystallinity of chitin.

In addition, the acidity of DES can contribute to the hydrolysis of the amorphous regions without any destructive effect on the crystalline areas of chitin structure. In other words, DESs can lead the chitin structure to acquire less amorphous and higher crystallinity construction.

XRD analysis of betaine-oxalic acid-DES-prepared chitin presented that the crystallinity of chitin decreased from 51.76 to 38.82% compared to intact chitin, which was associated with the splitting of intra- and intermolecular hydrogen bonds and the production of amorphous chitin after the treatment of chitin surface by DES solutions. According to TG analysis, lactic acid and butyric acid DESs-based chitins displayed lower thermal stability in comparison to pure chitin as a result of the lower molecular weight of DES-based chitin. Chitin treated with lactic acid and butyric acid DESs exhibited bigger pore sizes compared to the pure and acid/alkali-extracted chitin (Zhou et al., 2019).

When P-toluenesulfonic acid/ChCl (PTA-ChCl) DES was used to produce chitin nanocrystals, the crystallinity of pristine chitin and PTA-ChCl DES-treated nanocrystals chitin showed similar outcomes, while SEM images revealed that the chitin structure owned an irregular morphology as opposed to nanocrystals including PTA-ChCl DES with regular and rod-like shape structure. The sizes of 293.4 nm and 26.6 nm were calculated for the length and width of PTA-ChCl DES-treated nanocrystals chitin, respectively (Jiang et al., 2020).

XRD pattern proved that ChCl-malonic acid-based produced chitin possessed lower crystallinity in comparison to pure chitin as opposed to other (ChCl–thiourea, ChCl–urea, ChCl–glycerol) DES-based chitins, showing equal crystallinity compared to pristine chitin. $CaCO_3$ is an inorganic constituent of lobster shells in the chitin structure. The ChCl-malonic acid-based chitin displayed lower crystallinity contrasted to pure chitin, which was attributed to the vanished peak related to $CaCO_3$ in XRD results. The acidity of ChCl-malonic acid removed $CaCO_3$ from the chitin structure, which caused the crack of intra-and intermolecular hydrogen bonds. This crack led to the generation of an amorphous

chitin structure with a tiny lower crystallinity. TGA analysis demonstrated that the thermostability of chitin is dischargeable when extracted by DES. The extreme degradation temperatures of chitin samples were observed at the temperature of 349 °C. SEM images pictured the smaller particle size of DES-based chitin compared to pure chitin. The smaller particle sizes of chitin were caused by the easier dissolution of chitin in the DES (Zhu et al., 2017). ChCl-thiourea DES was utilized to produce chitin nanofibers, as strengthening fillers for calcium alginate beads. DESs can eliminate minerals and proteins in the chitin extraction process, and consequently increase the smoothness of the chitin structure. The SEM images of DES-treated chitin indicated slimmer and unaggregated nanofibers compared to untreated chitin with agglomerated structure. The chitin nanofibers produced by DES presented a higher yield (ca. 84%) in contrast to H_2SO_4-produced chitin nanofibers. Interestingly, NMR analysis was in agreement with the XRD pattern that revealed the attendance of carbonyl band of the amide of chitin in all DES-based chitin nanofibers, this testified the preservation of chitin structure after incorporation with DES precursors. Chitin nanofibers prepared by DES solution offered lower width (between 25 and 45 nm) and higher length (between 163 and 450 nm) compared with H_2SO_4-prepared chitin. The lower width and higher length could be more suitable in the construction of nanofibers (Mukesh et al., 2014).

ChCl, as HBA, and different HBDs (malonic acid, malic acid, lactic acid, levulinic acid) revealed crystallinity values in chitin samples of 87.48%, 79.82%, 82.21%, 81.27%, and 84.56% values for pure chitin, ChCl-malonic acid, ChCl-malic acid, ChCl-lactic acid, ChCl-levulinic acid, respectively. The results disclosed the minimal difference between DES-based chitin and pure chitin. TG analysis confirmed higher thermal stability of pure chitin in comparison to other DES-based chitin, which can be described by the higher molecular weight and crystallinity of pure chitin. SEM images implied the larger pore size in the DES-based chitin structure compared to other conventional chemically extracted chitin, which was attributed to the hydrolysis of produced chitin under the high acidity of the DES mixture. DES reduced the ash content in the chitin production process because of lessening calcium carbonate and other minerals from the raw material, which results in remaining the original morphology of chitin (Fig. 5) (Hong et al., 2018).

Wong et al. prepared chitin films using ChCl-urea, to increase the crystallinity and thermal stability of prepared DES-based chitin films, and compare them to the standard chitin. High dispersion of chitin without aggregation was cited as the main reason for the high crystallinity of chitin film prepared by DES, which formed the high thermal stability of chitin film. DES as a solvent for chitin preparation was preferred over other conventional solvents because of the high biodegradability, high crystallinity, and thermal stability of resulting DES-chitin films (Ramírez-Wong et al., 2016). Also, ChCl-lactic acid and betaine-glycerol increased the disruption of chitin's robust hydrogen bonding and facilitated the NaOH penetration compared with ChCl-oxalic acid DES, which generated higher deacetylation and dissolution. The high degree of deacetylation (80%) was comparable with other conventional methods for chitin extraction (Vicente et al., 2020). α-Chitin was dissolved in different DESs, including ChCl-urea, ChCl-thiourea, and betaine hydrochloride-urea, by Sharma et al. (M. Sharma et al., 2013), who noticed that ChCl-thiourea-based chitin displayed a more regular distribution of fibers with a homogeneous macrostructure contrasted to other DES-based chitin fibers. According to Sharma's analysis, the crystallinity of the chitin structure was disrupted in the DES mixture, which was associated with the breaking of the hydrogen bonds, resulting in a better chitin dissolution (M. Sharma et al., 2013). Chitin originated from shrimp shell was extracted using ChCl-malonic acid DES to prepare chitin films. DES-based and pristine chitin films displayed heavily dimpled, some coarse and extremely fibrous structures on their clave surfaces, illuminating an analogous arrangement of chitin. This was associated with N—H···OC hydrogen bonds connected to the parallel chitin chains by the amide groups. (Saravana et al., 2018). Ferric chloride hexahydrate and betaine chloride were mixed with chitin to form chitin nanocrystals. The average diameter, length, and crystallinity of chitin nanocrystals were calculated at about 10 nm, 268 nm, and 89.2%, respectively. Interestingly, a rod-like morphology was observed for chitin nanocrystals, which were compared to the attained *O*-acetylation chitin nanocrystals. The outcomes declared that the acetyl groups of attained *O*-acetylation chitin nanocrystals weaken the hydrogen-bonded crystalline structure of chitin and reduce the crystallinity of nanocrystals evaluated with DES-extracted chitins (Hong et al., 2020).

In conclusion, the molecular chains of the chitin structure were oriented in an antiparallel arrangement, which can cause the construction of a thermodynamically stable grid, reinforced by plentiful hydrogen bonds. DESs can be divided as good (ChCl-thiourea, ChCl–urea, ChCl–glycerol) and poor (ChCl–malonic acid) solvents considering their capability in changing the number of hydrogen bonding of chitin. The less disruption of hydrogen bonds guarantees more stable chitin in terms of thermal and mechanical properties. The resulting DES-chitin structure with more hydrogen bonds can be ascribed by the appropriateness of DES solvent for chitin extraction, which results in a chitin network with higher thermal stability, mechanical strength, and crys-

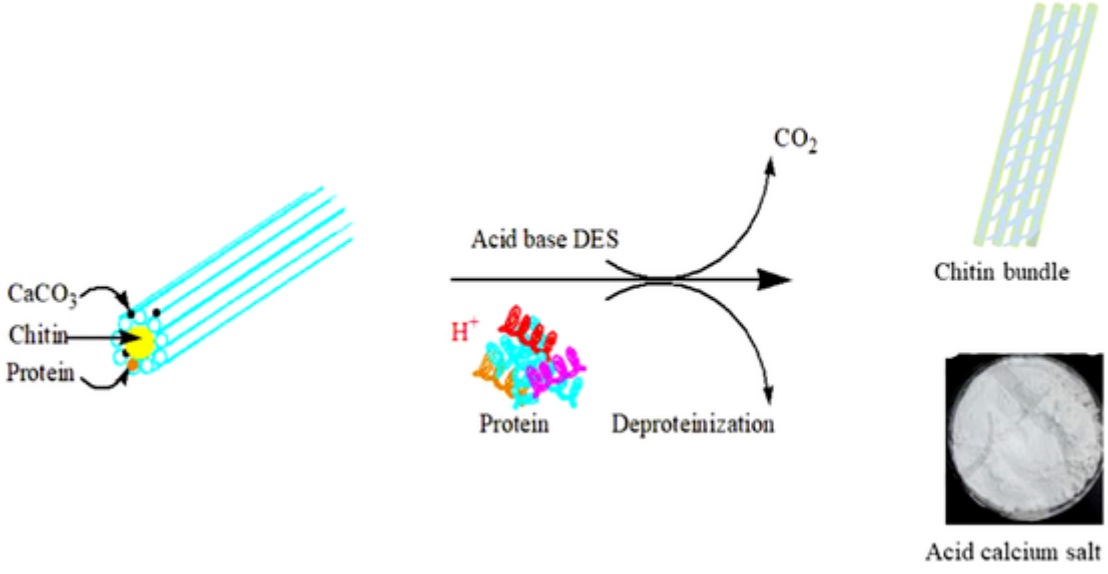

Fig. 5. Chitin isolation from lobster shell powder using DES (Hong et al., 2018) (License number 5040650130565).

tallinity. Stacking sheets of chitin structure in the good solvents partially vanished with a molecular distribution of chitin chains. The peeling of the molecular chain of chitin structure in bad solvents was not detected. Inappropriate DES solvent for chitin causes the cleavage of hydrogen bonds (OH…O) and the separation of a crystal into blocks. The thermal stability of DES-based chitin depends on its crystallinity. The higher crystallinity of DES-based chitin structure is related to higher thermal stability. Also, the pore size of DES-based chitin can be larger than pure chitin out of consideration the hydrolysis of chitin under harsh acid circumstances in the production process of chitin.

3. Chitosan

Chitosan, as biopolymer and polysaccharide, contains *N*-acetyl D-glucosamine and D-glucosamine units, which can be produced from the deacetylation of chitin (Khajavian et al., 2020a, b). Chitosan is identified as the soluble form of chitin, and it has been used in many industries, such as food packaging (Díaz-Montes and Castro-Muñoz, 2021a, b) and membrane technologies (Castro-Muñoz & González-Valdez, 2019), in different forms like film, since it exhibits superior features, including biodegradability, non-toxicity, functionality, biocompatibility, cost-effectivity, and availability in nature (Zinadini et al., 2014). As previously introduced, the low mechanical stability and weak plasticity generally limit the development and consolidation of chitosan films. The use of synthetic polymers and DES in the chitosan network can upregulate the mechanical strength of chitosan films. However, synthetic polymers, like polyvinyl alcohol as the best choice in the synthetic polymeric utilization approach, cannot increase the mechanical strength of chitosan films high enough to industrialize the chitosan films (Vatanpour, Salehi, Sahebjamee, & Ashrafi, 2018). Also, the discharge of synthetic polymers from the synthetic polymer-prepared chitosan films can decrease the biocompatibility features of produced chitosan film. DESs, as the new alternative for synthetic polymers in the chitosan structure, can be employed to not only increase the mechanical stability of chitosan film, but also the plasticity. High mechanical stability and plasticity can be valuable in the membrane and food packaging industries, respectively. In the case of food packaging, chitosan has been highlighted within the alternatives of "green packaging" (Hosseini & Gómez-Guillén, 2018), becoming more attractive when blended with nutraceutical compounds (Díaz-Montes and Castro-Muñoz, 2021a, b; Martins, Cerqueira, & Vicente, 2012).

3.1. Chitosan film production using DESs

Chitosan is the *N*-deacetylated derivative of chitin with a distinctive degree of acetylation between 0 and 50%. The crustacean shells, as the abundant sources of chitin, can be commercially used to produce chitosan. Chitosan structure includes plenty of amino and hydroxyl functional groups. The amino functionality of chitosan can cause various chemical reactions, including acetylation, quaternization, and specific interactions in aldehydes and ketones alkylation, grafting, chelation of metals, which result in the production of various interesting materials displaying several properties, such as antimicrobial, anti-acid, antiulcer, non-toxic, non-allergenic, total biocompatibility and biodegradability, etc. Furthermore, the hydroxyl functional groups of chitosan can facilitate several chemical interactions containing, *o*-acetylation, H-bonding, grafting, etc. (Pillai, Paul, & Sharma, 2009). Cost-effectivity and high adsorption capacity result in using chitosan-based films for heavy metal adsorption (Castro-Muñoz, Gontarek, & Figoli, 2019; Lasheen, El-Sherif, Tawfik, El-Wakeel, & El-Shahat, 2016). In addition, the food packaging industry has focused on using chitosan due to its good film-forming features, chemical stability, and high reactivity (Haghighi, Licciardello, Fava, Siesler, & Pulvirenti, 2020). Nevertheless, the low mechanical stability is referred to as the main intrinsic disadvantage of chitosan film. In this context, DESs can be utilized to raise the mechanical strength of chitosan films. The adding of DES can increase the plasticity and mechanical features of the chitosan films, as a result of a reduction in the stress and an increase in the elongation at break of prepared DES-chitosan film, respectively, compared to pristine chitosan film. Fig. 6 illustrates the changeable properties of chitosan films with the addition of DES into the chitosan matrix.

The chemical structure of HBD with different functional groups, such as one hydroxyl and carboxyl groups, can interact with the polymeric structure of chitosan (including also amino and hydroxyl groups) as a crosslinker or plasticizer agent, incrementing the mechanical stability of chitosan films via intermolecular binding. Intermolecular binding can be performed by covalent bonds that complement inherent intermolecular hydrogen bonds. Different strategies are cited to generate chitosan films including solution-casting (Castro-Muñoz et al., 2019), layer-by-layer (Castro-Muñoz, Agrawal, & Coronas, 2020), extrusion, thermo-compression molding, and solvent evaporation (Castro-Muñoz, 2020). The typical approach for the preparation of DES-chitosan films is the so-called solution-casting method that could involve solvent evaporation and is a straightforward and cost-effective method.

Very recently, chloride-malonic acid DES was proposed to plasticize the chitosan film using a solution casting method. For a better dissolution of chitosan, 2% w/v acetic acid was used and combined with DES (80 wt%), followed by stirring at 25 °C for 5 h to acquire complete homogenization. The DES-chitosan mixture was discharged into Petri dishes, and desiccated in an oven at 25 °C for 7 days which easily caused the creation of thin DES-chitosan films (Jakubowska et al., 2020). Almeida et al. (Almeida, Magalhães, Souza, & Gonçalves, 2018) also investigated the influence of ChCl-lactic acid and curcumin (as additive) for increasing the mechanical strength of the biopolymer films. Herein, ChCl and lactic acid with a molar ratio of 1:1 were mixed at 85 °C until a clear solution was detected and later cast. In general, it was found out that the films with DES displayed higher water vapor permeability, water solubility, and water sorption capability. Unfortunately, the embedding of the curcumin enhanced the barrier properties of the resulting films conducting to a reduction of water vapor permeability. Additionally, tensile strength was observed to be enhanced when using lower amounts of curcumin. The combination of ChCl-urea DES and chitosan carboxymethyl cellulose (Chitosan-CMC) mixture allowed to tailor a new DES/Chitosan-CMC membrane. Within the optimization, the specific amount of the chitosan (1 wt%) and CMC

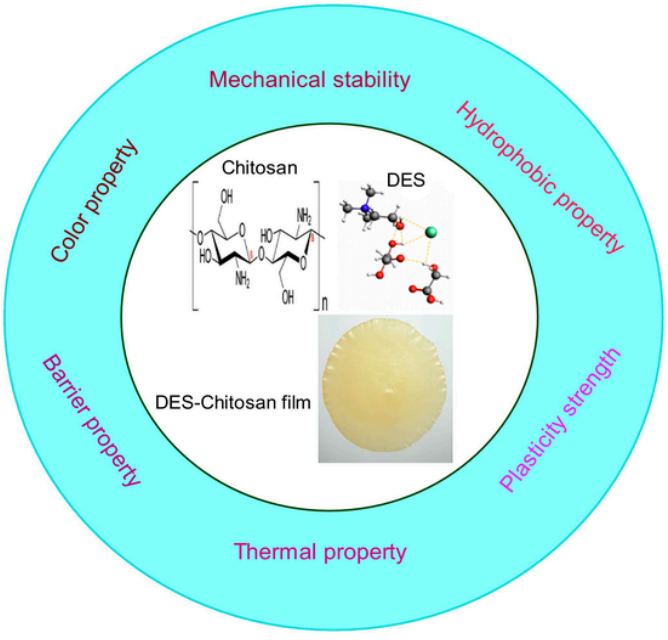

Fig. 6. Changeable properties of chitosan films with the addition of DES.

(1 wt%) were combined at room temperature. Subsequently, DES solution was added to the chitosan-CMC mixture with a proportion of 75:25. The above mixture (50 mL) was cast on a glass petri dish and put in an oven (60 °C). The dried membrane was washed with deionized water several times. The research demonstrated a positive outcome of the proton conductivity in the films without excessive swelling using DES compared with those without DES, with a small improvement in the thermal stability. (Wong, Wong, Walvekar, et al., 2018a).

DES was utilized to produce porous chitosan with tailored morphology in the absence of crosslinker, and in the form of film using a modified evaporation-induced phase separation process. 2% w/v solution of chitosan was acquired by mixing acetic acid aqueous (80% v/v) and correct amount of chitosan. The chitosan solution was stirred at room temperature to obtain a homogeneous solution. The DES solution was prepared by mixing ChCl and urea in the molar ratio of 1:2 at 80 °C to attain a uniform liquid. DES and chitosan solutions were mixed at 60 °C and cast with the optimum molar ratio of 1:1. Petri dishes and glass vials were utilized for the creation of films, respectively (Delgado-Rangel et al., 2020). Similarly, chitosan films were plasticized by ChCl-lactic acid DES, where chitosan powder was dissolved in acetic acid solution (49 mL of 2% w/v) and then mixed in the DES mixture (60 wt%). The DES-chitosan mixture was agitated at room temperature for 5 h until a fully homogenized solution was obtained. The uniform solution was transferred into the petri dish and dried in an oven at 25 °C for 7 days (Jakubowska et al., 2021). ChCl-urea DES was employed as an additive to increment the mechanical stability of chitosan film. DES solution was prepared by the combination of ChCl and urea (molar ratio of 1:2) in a nitrogen-purged bottle at the temperature of 120 °C for 4 h. The homogenous DES (1 wt%) solution was added to the chitosan solution, including 1 wt% of chitosan and 100 mL of 0.1 M acetic acid, and then agitated for 4 h at 47 °C. 50 mL of DES-chitosan solution was cast onto a petri dish and air-dried for 10 days. After the evaporation of acetic acid, the prepared films were dried in an oven for another 24 h at 60 °C to guarantee the comprehensive removal of DES. Dried films were washed by distilled water up to neutralized pH was achieved (Wong, Wong, Walvekar, et al., 2018b). The effect of DES, which was constructed by ChCl (HBA) including different HBD (malic acid, lactic acid, citric acid, and glycerol), on plasticizing of chitosan film was assessed for the food packaging applications. Dried chitosan particles (for 24 h at 60 °C) were mixed with the previously prepared DES mixture in the ratio of 70/30 for 15 min. The DESs-chitosan mixture was put into an oven at 80 °C for 30 min. Then, the mixture was combined with an aqueous acetic acid solution (3 wt%) for 15 min (chitosan/acetic acid solution: 25/75 w/w). 1 g of the chitosan-DES mixture was located in a circular mold (diameter = 5 cm and thickness = 2 mm). After removing the circular mold, the molded paste was protected with aluminum foil between two stainless steel plates and then thermo-compressed in a hydraulic press at 110 °C. Then, before removing from the foils, the hot chitosan films were cooled for 20 min (Galvis-Sánchez, Castro, Biernacki, Gonçalves, & Souza, 2018). The chitosan/DES films played as a supporting matrix for polypyrrole-based film electrodes in vapor phase polymerization of pyrrole. For the preparation of the chitosan-DES film, the chitosan powder was added to the ChCl-lactic acid (1/2 mol mol^{-1}) DES in the mass ratios of 1:4 (chitosan:DES). The combination of DES-chitosan was dissolved in deionized water in the concentration of 2 wt%. The mixture was agitated at 25 °C, then cast in petri dishes, and desiccated at room temperature (Vorobiov, Smirnov, Bobrova, & Sokolova, 2021). In a different approach, chitosan films were prepared by ChCl-citric acid DES by thermo-compression molding method. Chloride and citric acid (1:1) were mixed with chitosan for 15 min by pestle and mortar in optimum quantities, then heated in an oven at 70 °C for 30 min. The hot DES-chitosan paste was detached, and mixed with the aqueous acetic acid solution (3 wt%) for 15 min (Galvis-Sánchez, Sousa, Hilliou, Gonçalves, & Souza, 2016). The casting of the resulting dope solution was done as previously reported (Galvis-Sánchez et al., 2018). Microcrystalline cellulose (MCC) and ChCl:glycerol were combined with chitosan solution to increase the mechanical stability of chitosan film. Also, curcumin (1 w/v%) was added as the antibacterial activator. The optimized MMC/DES/chitosan mixture was dispensed on petri dishes and dried for 24 h (Pereira & Andrade, 2017). With a very similar strategy, a mixture based on ChCl (2.71 g) and malonic (2.32 g) was utilized to plasticize the chitosan structure. In addition, cellulose nanocrystals (CNC) were added to the DES-chitosan mixture as filler. The CNC/DES/chitosan mixture was agitated for 5 h and later cast on a glass surface with a thickness of 20 μm. Finally, CNC/DES/chitosan films were air-dried at 25 °C for 6 days (Smirnov et al., 2020). Until now, different strategies have been adopted by the research community, in which the casting method has been identified as the most versatile way for preparing DES-chitosan films. Table 2 summarizes the application and morphological effect of different DESs in the preparation of chitosan-based films. The table shows the food industry as the most applicable area for DES-based chitosan films.

3.2. Characterization of DES-chitosan films

Since it is well known that chitosan possesses a large number of amino and hydroxyl groups, the HBA and HBD of the DES can easily interact with polymer structure. Such interactions can change the chemistry and morphology of resulting DES-chitosan films compared with pristine chitosan film. Therefore, it is essential to study the chemistry of DES-chitosan structure using analysis (like FTIR) to visualize such interactions. The following subsection addresses the "chemistry" behind the chitosan and DESs reported in the literature.

Table 2
Different DESs used for the production of chitosan-based films.

HBA	HBD	Ratio	Morphology effect	Application	Ref.
ChCl	Malonic acid	1:1	Dense morphology, without any pores	Food packaging	(Jakubowska et al., 2020)
ChCl	Lactic acid	1:1	Uniform morphology, without visible holes or cracks	Food packaging	(Almeida et al., 2018)
ChCl	Urea	1:2	Less brittle and more flexible	Film	(Wong, Wong, Walvekar, et al., 2018b)
ChCl	Urea	1:2	Higher degree and homogeneously dispersed of porosity	Production of monoliths and films	(Delgado-Rangel et al., 2020)
ChCl	Lactic acid	1:1	Rough	Food packaging	(Jakubowska et al., 2021)
ChCl	Malic acid	1:1	Non-homogenous	Food packaging	(Galvis-Sánchez et al., 2018)
ChCl	Lactic acid	1:1	Non-homogenous	Food packaging	(Galvis-Sánchez et al., 2018)
ChCl	Citric acid	1:1	Homogenous and smooth	Food packaging	(Galvis-Sánchez et al., 2018)
ChCl	Glycerol	1:2	Heterogeneous domains with voids	Food packaging	(Galvis-Sánchez et al., 2018)
ChCl	Lactic acid	1:4	Wrinkled surface morphology	Potential separator for electrochemical energy storage devices.	(Vorobiov et al., 2021)
ChCl	Malonic acid	1:1	Increased elongation at break	Film	(Smirnov et al., 2020)
ChCl	Glycerol	1:1	Smooth morphology	Food packaging	(Pereira & Andrade, 2017)

3.2.1. Chemical properties of DES-based chitosan film structures

Chitosan has been introduced as a strong base as a result of the existence of the amino groups (Salehi et al., 2012). In principle, chitosan can be solubilized in an acidic environment (below pH 6.0), in which chitosan's amines are deprotonated and the polymer loses its charge and thus converts it to an insoluble form (Haghighi et al., 2020). Also, the chitosan can be solubilized, depending on the ratio between both units D-glucosamine and *N*-acetyl-D-glucosamine, if the deacetylation degree touches 50%. Chitosan is more soluble than chitin that is attributed to the $-NH_2$ bond protonation on the C-2 location of the D-glucosamine repeat unit containing the alteration of polysaccharide to polyelectrolyte in the pH below 6 (Akyuz et al., 2017).

On the other hand, many strategies have been utilized to improve the different features of chitosan film, comprising mechanical and thermal stability, water vapor permeability, biodegradability, and crystallinity (Sharma, Sharma, & Jain, 2021). The incorporation of DES into the chitosan is the most superior approach to enhance the aforementioned features of chitosan-based films. The components of DES can cooperate with chitosan structure, resulting in a crosslinking and therefore enhancing its functionality, together with mechanical and thermal stability. The carboxyl groups of particular DES can interact with the amino groups of chitosan creating an amide connection, which leads to a higher crosslink feature of DES-chitosan films compared with pristine chitosan. Hence, the cross-linking protocol enhances the mechanical stability of chitosan produced by DES. Moreover, chitosan-DES interactions can affect the creation of chromophore molecules, and change the color of prepared DES-chitosan film. A high amount of hydroxyl groups in the DES can increase the interaction between amino groups of chitosan and –OH groups of DES (Guerrero, Muxika, Zarandona, & de la Caba, 2019).

FTIR analysis displayed particular alterations in the chemistry of chitosan films after mixing with ChCl-malonic acid DES. Considerable variations (1600–1530 cm^{-1}) compared to pure chitosan films, revealed the existence of amide I (C═O stretching) and amide II (C—N stretching and C—N—H bending vibrations) bands in the structure of DES-chitosan. The new stretching of C═O groups in the polymeric matrix of DES-chitosan films was detected at 1720 cm^{-1}, which was attributed to the carboxylic groups characteristic of HBD, malonic acid. The intensity of 1480 cm^{-1} (CH_2 bending) and at 950 cm^{-1} bands related to DES in the DES-chitosan films, rose with an increase in the DES amount. The increased amount of DES contributed to a more heterogeneous structure of DES-chitosan films. Also, the more degree of deacetylation of chitosan meant more homogenous surface structure. A higher degree of deacetylation of chitosan means the higher difference in the quantity of hydrophilic functional groups (OH and NH_2), which leads to an increase in the robustness of hydrogen bonds between adjacent macromolecules. The reinforced hydrogen bonds improve the plasticization process of chitosan film (Jakubowska et al., 2020).

FTIR clarifications proved the increase of intermolecular hydrogen bonds between ChCl-urea DES and chitosan because of the increased amount of DES. The amide groups of urea led to firm hydrogen bonding with the chloride anions of ChCl, and OH and NH_2 groups of chitosan, simultaneously (Delgado-Rangel et al., 2020). The majority of bands characteristic of the pure chitosan was revealed in the FTIR analysis of chitosan films prepared by ChCl-lactic acid DES. The number of O—H and N—H vibrations (3700–3000 cm^{-1}) involved in the creation of H-bonds between constituents, including chitosan, DES, and water, increased with upregulating DES content. The hydrogen and ionic bonds were dominant interactions in the structure of DES-chitosan film (Jakubowska et al., 2021). FTIR results declared that the incorporation of ChCl-urea DES into the chitosan structure was able to create the saccharide ring (C—O—C) between DES and chitosan, which approved effectively the formation of a resilient solid biopolymer membrane without adding cross-linking mediator (Wong, Wong, Walvekar, et al., 2018b). The combination of ChCl-citric acid DES and chitosan showed films with higher smoothness and more homogenous surface compared to other DES-chitosan mixtures. The amide I and the amide II bands of the protonated amide group were observed for all DES-chitosan films in the FTIR outcomes (Galvis-Sánchez et al., 2018). The chemical analysis displayed that the cellulose molecules had an affinity to be dissolved in the ChCl-urea DES structure and less incorporated into the hydrogen-bond network (Smirnov et al., 2020).

As a conclusion for the chemistry of DES-chitosan films, the amide I (C═O stretching) and amide II (C—N stretching and C—N—H bending vibrations) bands appeared in the chitosan structure after the incorporation of DES into the chitosan films. The C═O groups of DES-chitosan films were attributed to the carboxylic groups that are characteristic of HBD (e.g., malonic acid). The strength of CH_2 bending upregulated with the increased amount of DES into the chitosan structure. The higher degree of deacetylation of chitosan proved the higher difference in the quantity of hydrophilic functional groups (OH and NH_2), which causes the differences in the number and robustness of hydrogen bonds between adjacent macromolecules and being responsible for the plasticizing effect of DES. The quantity of O—H and N—H bonds tackled in the formation of H-bonds, as dominant interaction in the DES-chitosan films, increased with upregulating DES content. To some extent, it can be stated that more hydrogen bond means more mechanical and thermal stability of chitosan films. Fig. 7 displays the influence of DES on the chitosan film structure. The DES-based chitosan film plasticization was performed by creating connections between hydrogen bindings of chitosan chains and the hydrogen bond-dominated structure of DES.

3.2.2. Morphology of DES-based chitosan film structures

Superior features of chitosan, including biodegradability, antibacterial ability, film-forming ability, renewability, absorbability, nontoxicity, are cited as the main attributes for producing chitosan-based films (Kalaycıoğlu, Torlak, Akın-Evingür, Özen, & Erim, 2017). The low mechanical stability, which is in direct proportion with the molecular weight and deacetylation degree of chitosan, is the main drawback of chitosan films (Mujtaba et al., 2019). Some studies exhibited that the mechanical properties of chitosan can be improved by the incorporation of DESs into the chitosan films. Elongation at break (*Eb*), tensile strength (*TS*), and Young's modulus (*YM*) values are certainly announced as the main measurements for evaluating mechanical properties of prepared films, in which the increased elongation at break can upregulate the mechanical strength of chitosan films. A better elongation at break is translated to less film rupture. Furthermore, the proper crosslink of chitosan structure using DESs can enhance the mechanical strength of chitosan film. The possibility of the crosslinking process of chitosan via DESs can be divided into the different strategies, including (i) covalent amide/imine linkage, (ii) metal–protein complex formation, (iii) H-bond formation (between –OH group with different types of amino acids)(Qiao, Ma, Zhang, & Yao, 2017). Moreover, DES can reduce the accumulation of particles in the polymeric structure of chitosan, which can be attributed to the enhanced mechanical stability of the chitosan monosaccharides, as a result of robust hydrogen bonds between DES components, and the hydroxyl and amine groups of chitosan. Moreover, DES can be employed to plasticize the chitosan film structure, practicalizing the usage of chitosan films in the food industry. In theory, a plasticizer can be described as an additive that when combined into the polymer can increase the flexibility, workability, and distensibility, and decrease the brittleness of the prepared polymer. DES can decrease the tension of deformation, hardness, density, viscosity, and electrostatic charge of chitosan films, simultaneously, which result in high plasticity and superior features including flexibility, resistance to fracture and dielectric constant. In addition to this, particular properties, such as transparency, thermal stability, the smoothness of surface, and water vapor transmission ability, can be enhanced utilizing DES.

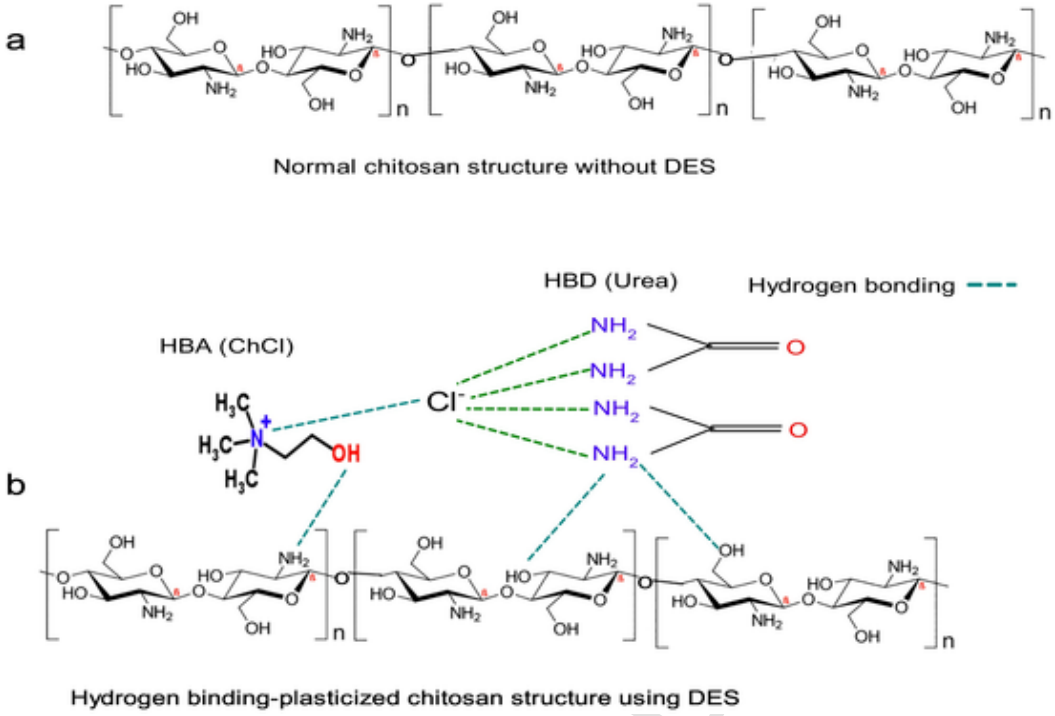

Fig. 7. Chitosan structure a) before the incorporation of DES (ChCl-Urea), b) after incorporation of DES (HBA + HBD) and plasticization process.

The ChCl-malonic acid DES was mixed with chitosan film to apply it in the food packaging industry. Thermogravimetric analysis revealed that the thermal stability of chitosan films decreased after combination with DES, out of consideration of the loss of absorbed water bound to the hydroxyl and amino groups of chitosan by fragile hydrogen connections. The temperature of 125 °C was recorded as the first point in which the weight loss process was befalling. The outcomes indicated that the higher amount of DES in chitosan films means the higher mass loss, which caused a reduction of thermal stability of chitosan films. This reduction in thermal stability was ascribed to the malonic acid decomposition, because of the decarboxylation of malonic acid. SEM analysis proved that the uniform and very smooth surface of pristine chitosan films turn into a heterogeneous surface with dense morphology and without any pores of DES-chitosan film, out of the consideration of existing of DES with low molecular weight in the chitosan structure. According to AFM analysis, when DES content exceeded 60 wt%, the roughness of DES-chitosan films increased by adding DES. DES-chitosan films with 70–80% displayed smoother surface compared to DES-chitosan film with 50 wt% DES, which was attributed to the penetration of DES components into the chitosan matrix and thus the disruption of inter-and intramolecular hydrogen bonds. Furthermore, the incorporation of DES into the chitosan structure caused a more continuous and plasticized phase of DES-chitosan films. The low amount of DES in a DES-chitosan film cannot fill the entire space between chitosan macromolecules, which leads to nodules in the film structure. Uplifting the amount of DES resulted in growing the ball-shaped nodules and shaping the continuous phase with macromolecules. When DES content in the DES-chitosan film increased, the thickness of the film obeyed the degree of deacetylation of chitosan. Differently from previous reports, tensile strength analysis revealed that the addition of DES into the chitosan films contributed to reducing the mechanical stability of films with a more rigid structure because the higher amount of acetyl groups (lower degree of deacetylation) tends to create more intermolecular hydrogen bonds, reducing the plasticity of DES-chitosan films thanks to the higher intermolecular interaction. The color of films employed in the food packaging industry is defined as one of the crucial factors for prepared material. At this point, translucent materials are more preferred for the food packaging industry due to the better appearance and shelf presence of the product. In the conventional method, like thermo-compression molding, the color of DES-incorporated chitosan films tends to become yellow, which was undesirable. However, the solvent evaporation technique could produce DES-chitosan films with high translucent compared to conventional methods. Importantly, water vapor transmission rate (WVTR) is another important factor in the food packaging industry. The value or range of WVTR relies on the product, which is aimed to be protected. Unfortunately, there is no defined parameter to evaluate the appropriateness of a produced film considering this WVTR. The incorporation of DES into the chitosan film increased the WVTR of film out of consideration of the high hydrophilicity of DES used as a plasticizer in the chitosan construction (Jakubowska et al., 2020). It is important to point out that hydrophilic chitosan-DES material could be suitable for specific selective membranes technologies (such as pervaporation), which are commonly used in the removal of polar compounds from azeotropic mixtures (Castro-Muñoz, Galiano, & Figoli, 2020; Castro-Muñoz & Boczkaj, 2021).

ChCl-lactic acid DES was synthesized and later evaluated to increase the plasticity of chitosan films, together with the visual appearance and optical properties. The surface of DES-chitosan films displayed a yellowish, uniform, semi-translucent, and malleable surface. A surface without pores, cracks or insoluble particles, proved well-prepared films to be used in the food packaging industry. In the SEM images, small particles inside the compacted DES-chitosan films were observed caused by the incorporation of DES. The tensile strength of chitosan films decreased when increasing the amount of DES, which was related to the fact that the movements of polymer chains were eased when the structure of DES-chitosan film becomes less dense; unlike pure chitosan film, a freer volume in the DES-chitosan films was noted. The hydrophilic features of DES used in chitosan films also raised the water vapor diffusion water solubility of DES-chitosan films (Almeida et al., 2018).

Wong, Wong, Rashmi, and Khalid (2018) performed the characterization of ChCl and urea (DES)/CMC membrane. The embedding of DES between the polymeric chains of CMC and chitosan caused an increment in the thickness of DES/CMC/chitosan membranes. SEM images exhibited that the DES addition upregulates the intramolecular

hydrogen bonding between chitosan and CMC polymer, which contributes to a smoother with almost negligible agglomeration on the chitosan membrane surface.

The robust ionic interaction of oppositely charged ions between DES and the polymeric chains of chitosan-based membrane increased the mechanical stability, proton conductivity, polymer chains flexibility of membrane, and more particularly, avoided the polymer in the solid form to be dissolved in water. The hydrogen bond interactions between the C—O groups of chitosan with urea in DES were explained as the plasticizing effect of DES. The high proton conductivity of DES-plasticized chitosan membrane was ascribed to the existence of DES, which resulted in a reduction of the crystallinity of DES-chitosan membrane contrasted to the pristine chitosan membrane. The reduced crystallinity was attributed to the broken-hydrogen bonds between amino groups and hydroxyl groups by complexation, which caused higher amorphousness in the DES-chitosan membrane in comparison to the pristine chitosan membrane. DES also enhanced the thermal stability of Chitosan-CMC blend films (Wong, Wong, Rashmi, & Khalid, 2018).

In recent work, ChCl-urea DES was once again evaluated to construct chitosan films. The higher quantities of DES in the chitosan structure provoked to amalgamate smaller pores and consequently produced larger pores. The DES-chitosan samples, containing high DES quantity, can contribute to creating large irregular areas by the removing of the additional DES from the network at the evaporation process. For instance, a high chitosan ratio in comparison to DES (chitosan/DES 3:1) avoided the creation of pores and instigated a porous free film structure. The flow of the DES in small domains through the chitosan matrix formed holes, which were left behind after the removal of DES by acetic acid without extraction of insoluble chitosan (Fig. 8). Upregulating the amount of chitosan in proportion to DES amount, reduced the swelling capacity of the DES-chitosan membrane, which was described by the restricted swelling of the polymer as a result of a dense chitosan network (Delgado-Rangel et al., 2020).

When Jakubowska et al. employed ChCl-lactic acid DES to increase the plasticity of the chitosan films, the SEM images of DES-chitosan films showed uniform morphology without noticeable holes or cracks, similar to the pristine chitosan films, which was associated with the hydrogen connections, and interactions between protonated amino groups of chitosan and carboxylate groups of lactic acid because of the compatibility between both substrates. On the other hand, AFM analysis exhibited that the excessive amount of DES (<60%) into the polymeric matrix of chitosan can create micro intrusions of different phases and higher surface roughness in the DES-chitosan films. The increased amount of DES in the chitosan films uplifts the water vapor absorption process, which contributed to an increased thickness of the DES-chitosan films contrasted to the pure chitosan film. Thermal stability of DES-chitosan films decreased with rising the amount of DES because the water bonds tend to discontinue their connection to the hydroxyl and amino groups of the chitosan structure, creating a connection with components of the high hydrophilic structure of DES. The tensile strength of DES-chitosan films also decreased by rising the DES amounts. However, the tensile strength tests disclosed that the mechanical stability of DES-chitosan films depends on the DDA of chitosan. The chitosan, presenting DDA around 95%, can improve the mechanical stability by three times higher than chitosan with DDA of 70% using the similar amount of DES. The mechanical features were credited to the dissimilarity in the number of amino groups accountable for H-bonds creation, controlling the rigorousness of the pristine and plasticized polymer network of chitosan. The incorporation of DES into the chitosan structure led to the homogenous and semi-transparent surface with a slight yellowish tint, and without visible holes, which was approved by surface color measurements. It was concluded that DES components and chitosan sources (shrimps waste in this case) can affect the transparency of DES-chitosan films (Jakubowska et al., 2021).

By adding ChCl-urea DES, Wong and his colleagues proposed the enhancement of the elongation at the break of chitosan films. At this point, the DES increased the elongation at break and flexibility of DES-chitosan film and reduced the aggregation of particles in the chitosan structure, which was ascribed to the improved polymerization of the chitosan monosaccharides, as a result of robust hydrogen bonds between DES components and the hydroxyl and amine groups of chitosan. The ionic conductivities of the DES-chitosan films were also evaluated by complex electrochemical impedance spectroscopy. The increment of DES into the chitosan increased the ion conduction through the resulting DES-chitosan films, which was attributed to the existence of mobile ions in the hydrated state that contribute to the conduction process

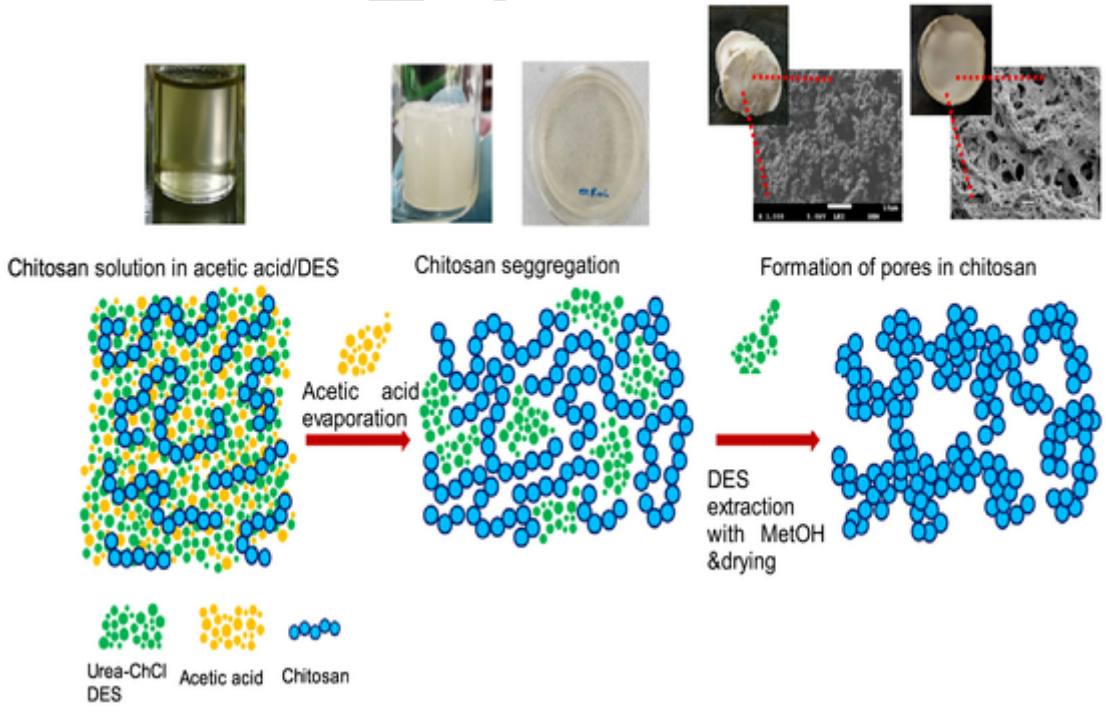

Fig. 8. Creation of porous chitosan using DES solvent (Delgado-Rangel et al., 2020) (License number 5040660197457).

(Wong, Wong, Rashmi, & Khalid, 2018). As demonstrated by Wong, Wong, Rashmi, and Khalid (2018), Galvis-Sánchez et al. (2018) documented that ChCl-citric acid DES-chitosan film proved the highest elongation at break compared with other DES-chitosan film, which was in agreement with SEM results presenting the most homogeneous surface and compact structure. This was qualified by the highest amount of carboxyl groups in the citric acid compared with other HBDs (e.g., malic, lactic acids). The higher carboxyl groups in the DESs, like the ones provided by citric acid, may favor a more and stronger hydrogen bond between –OH groups of chitosan and DES structure, as a result of the existence of the adjacent carbonyl moiety. It was highlighted that the interaction between DES and chitosan structure has relied on the accessibility of H_{OH} hydrogen of the DES as the plasticizer. In the same study, the water vapor permeability of chitosan films exhibited an increase with the addition of ChCl-glycerol DES due to the fact that glycerol molecules could be placed between adjacent chitosan chains, and hence decrease the intermolecular attractions that caused the easy transport of water vapor molecules. The moisture barrier property of film was enhanced by the addition of DES into the chitosan film, owning to the hydrophilic structure of DES, which results in adsorbing higher quantities of water at high humidity circumstances (Galvis-Sánchez et al., 2018).

Vorobiov and his coworkers entangled a ChCl/lactic acid-based polymer electrolyte into the chitosan structure, as a separator for electrochemical energy storage devices. The conductive features of chitosan increased with the introduction of DES into the chitosan out of consideration of increased charge carrier density in the film (Vorobiov et al., 2021). Thermo-compression molding methodology was employed to prepare chitosan films using ChCl-citric acid DES. Some aggregations were observed in the ChCl-citric acid/chitosan films in the compression molding method compared to the films prepared by acetic acid as a solvent for chitosan, which was attributed to the reorganization of chitosan molecules caused by the interaction between citric acid of DES and acetic acid used for chitosan dissolution. Also, the result of the WVP demonstrated that it can be affected by different parameters, including chitosan molecular weight, type and concentration of DES, and film preparation technique. The interaction between the polysaccharide and DES formed the slight interstitial spaces between the polymeric matrixes and increased the permeation rate of DES-chitosan films. Thermal stability outcomes displayed that the thermal degradation of DES-chitosan occurred earlier compared to pristine chitosan at 200 °C. The opacity feature of chitosan films improved by the incorporation of DES into the chitosan films which was associated with the higher thickness values of DES-chitosan films. Maillard reactions, which were described as the color alterations that occurred in the duration of the thermo-compression molding of chitosan films as non-enzymatic browning reactions, was occurred in the preparation of chitosan film using DES (Galvis-Sánchez et al., 2016). Pereira and his colleagues incorporated ChCl-glycerol DES into the chitosan construction. In this way, DES contributed to the better homogenization of the polymeric structure of chitosan with smooth morphology and higher tensile strength of DES-chitosan surface (Pereira & Andrade, 2017). Cellulose nanocrystals (CNC) and ChCl-urea DES were utilized in the chitosan films to improve their morphology features.

The crystallinity of chitosan films is determined by the quantity of the intra and intermolecular hydrogen bonds broken by DESs in the dissolution process. More disruption of the intra and intermolecular hydrogen bonds means less crystallinity. The crystallinity of chitosan did not change after the incorporation of DES but contributing to better solubilize cellulose macromolecules contrasted to water according to better destruction of H-bonds. In addition, the reactions between –OH groups of CNC, and the constituents of the CS/DES mixture, led to the increased elongation at break. The interaction between the urea C═O group and chloride ions of DES and hydroxyl groups of cellulose destroyed CNC particles in the solvation process (Smirnov et al., 2020).

According to the current development works, it can be preliminarily concluded that DES, as an additive, can significantly increase the plasticity and mechanical stability (especially elongation at break) of chitosan films. In principle, DES can lower the tension of deformation, hardness, viscosity, and the electrostatic charge of chitosan polymer, which contribute to the chitosan films with more flexibility, resistance to fracture, and plasticity compared to pristine film. On the other hand, DESs can increase the elongation at the break of the chitosan membrane, as one of the measurements for mechanical stability evaluation. The increment of elongation at the break by upregulating DES can be attributed to the increased free volume in the polymer matrix, which results in an expansion of a free volume promotion of polymer chains translation, which is vital to the steadiness of the film in the elastic flow regime of deformation. Also, the existence of DES in the chitosan structure decreases the tensile strength and crystallinity, while increasing the smoothness of chitosan construction. A reduction in the tensile strength of chitosan after incorporation of DES can be ascribed to the fact that the higher amount of acetyl groups or lower degree of deacetylation tends to create more intermolecular hydrogen bonds, which in turn reduces the tensile strength of DES-chitosan films due to the more intermolecular interaction. However, carboxyl groups in DES structure can provide the stronger hydrogen bond between -OH groups of chitosan according to the presence of the adjacent carbonyl moiety. Importantly, the hydrophilic structure of DES can also enhance the WVTR of the resulted chitosan film.

4. Other applications of DESs in chitosan structure

Apart from preparing chitosan film using DES solvents, these solvents can be smartly utilized for the chemical functionalization of chitosan, producing chitosan-based imprinted buildings, beads, and monoliths. In this section, the chemistry and characterization of these DES-incorporated chitosan structures will be discussed.

4.1. *N,N,N-trimethyl chitosan and DES*

N,N,N-trimethyl chitosan (TMC) is one of the derivatives of chitosan with high solubility at neutral and alkaline pH because of the perpetual positive charge on its amine group. Traditional solvents, including acetic acid, *N*-methyl-2-pyrrolidone (NMP), dimethyl sulfate (DMS), dimethyl formamide (DMF), can be used to prepare TMC. However, low selective *N*-methylation, low productivity, and hazardous materials involved in the TMC preparation are quoted as the weaknesses of produced TMC by traditional solvents. Here, DES can enhance biodegradability, productivity, non-toxicity, and thermal strength, low flammability of DES-prepared TMC compared with other TMC prepared by conventional methods.

Bangde and his coworkers incorporated DES into the amine groups of chitosan to produce trimethylated, di-methylated and monomethylated polymer. Experimentally, chitosan was added to the mixture including DMF:H_2O (1:1; v:v; 20 mL), and then poured into methyl iodide with fixed alkaline settings by 0.5%. ChCl-urea DES was mixed with chitosan mixture (300 rpm) at 25 °C for 48 h. The methylated chitosan was centrifuged after the precipitation of the DES-chitosan mixture at the adjusted pH of 9 by 0.1 N NaOH. The centrifuged methylated was rinsed several times by acetone, and freeze-dried to acquire water-soluble white powder. The attendance of methylated chitosan peaks (1630–1660 cm^{-1}) proved the characteristic absorption of the N—CH_3 bond as a result of the quaternary ammonium group (1415–1430 cm^{-1}). The DES-chitosan showed superior methylated chitosan contrasted to other chemical methylation, which was attributed to the high selectivity of DES towards *N*-methylation in the DES-chitosan materials. ChCl-urea DES delivered mild alkaline circumstances, which caused generated methylated chitosan without degrading the parent polymer (Bangde, Jain, & Dandekar, 2016). In another

study, TMC was produced by dimethyl carbonate (DMC) in a reaction medium comprising of ternary deep eutectic solvents (TDES). TDES is typically known as a subclass of DES with the combination of three ingredients. In this work, TDES was synthesized by mixing ChCl, urea, and glycerol (1:2:2) at 80 °C, until a clear liquid was attained. TMC was produced as follows: chitosan (300 mg) was added in 0.5 mL of deionized water, 2 mL of TDES, 6 mL of methyl iodide, and 6 mL of 0.1 N NaOH. The final mixture was agitated in a pressure tube (at 1300 rpm, 60 °C) for 8 h. Then, the mixture was chilled at room temperature (27 °C) and then precipitated by acetone. After the centrifugation process, the chitosan powders were freeze-dried and preserved as fine powders. The resulting TDES showed a higher ability to activate enzymes (e.g., lipase) compared with other DES, which was related to the plenty of hydrogen bonding as hydrogen bond activators in the TDES structure. It was concluded that the methylation of chitosan was an interface phenomenon at the contact surface between TDES and DMC. The connectedness between TDES with catalyzed features and DMC increased the possible connection between the enzyme and the functional groups of chitosan and DMC. XRD outcomes (Fig. 9) revealed that the amorphous nature of TMC created new peaks in the chitosan structure after the methylation process of chitosan. Also, FTIR analysis proved that the angular deformation of the N—H bond of the amino group removes the functional amino group in the structure of *N,N,N*-trimethyl chitosan produced by DES-based solvents, compared to pure chitosan (Mahajan, Bangde, Dandekar, & Jain, 2020).

The production of TMC using DES can decrease organic reactant quantities, reaction time, and generate the methylated chitosan without influencing the molecular weight of the formed product. Therefore, DESs are effective and safe solvents to create TMC compared with harmful organic solvents.

4.2. Imprinted chitosan-based structures by DES

The molecular imprinting technique can be employed to prepare a cross-linked polymer matrix around an imprint molecule, which includes tailor-created attaching sites considering their shape, size, and functional groups for the accurate acknowledgment of exact biological and chemical moieties. The elimination of template molecules and functional monomers has been announced as the main disadvantage of traditional methods for producing imprinted structures, which result in decreasing the number of accessible sites. In a chitosan-based structure, molecularly imprinted chitosan by DES solvents has been proposed to eliminate the aforementioned disadvantages. DES was applied to manufacture molecular-imprinted magnetic chitosan (Fe_3O_4-CTS@DES-MIPs) to employ selective acknowledgment and removal of (+)-catechin, (−)-epicatechin, and (−)-epigallocatechin gallate in black tea. ChCl-methacrylic acid DES (1 mL), synthesized Fe_3O_4@chitosan (200 mg), ethylene glycol dimethacrylate (7.5 mmol), (+)-catechin (0.1 mmol), and methanol (4 mL) were mixed for 24 h at room temperature, which contributes to the creation of template and monomers. After the polymerization and saturation process, the polymer was crushed and sieved (105 μm) by mesh, followed by rinsed in methanol-acetic acid solution and dried at 60 °C. Fe_3O_4-CTS nanoparticles by the self-assembly of DES were employed to produce an imprinted and polymerized layer. DES presented a high capability to create hydrogen-bonding interaction between its construction and the target molecules, which caused the use of DES as a functional monomer. The vibrations of H-bondings, C—O, and C═O in the FTIR analysis were attributed to the presence of DES. The selective separation of prepared DES-based polymer proved high ability for the separation of (+)-catechin (ca. 95%), (−)-epicatechin (ca. 92%), and (−)-epigallocatechin gallate (ca. 90%), proposing DES as a functional monomer for selective bioactive combinations without interfering imprinting process (Ma, Dai, & Row, 2018). The molecularly imprinted chitosan microspheres-magnetic graphene oxide was produced using DES, which acted as a functional monomer

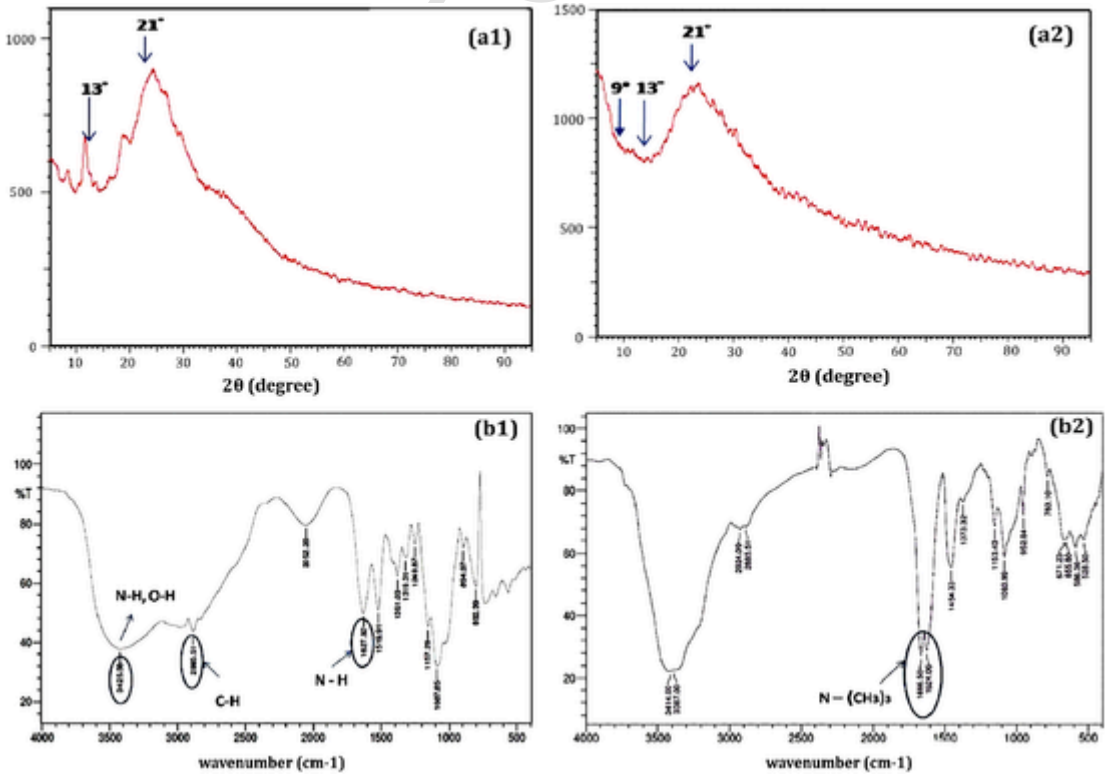

Fig. 9. The comparison of XRD and FTIR results of a1 and b1) pristine chitosan and, a2 and b2) *N,N,N*-trimethyl chitosan produced by DES-based solvents (Mahajan et al., 2020) (License 5039390333753).

and template, simultaneously. ChCl-2,4,6-trichlorophenol DES was selected as a solvent to provide imprinted structure. DES-related vibrations, including the vibration of –CN and the symmetrical vibration of NH, displayed an overlapped stretching vibration. The increment in specific surface area of the imprinted structure by DES compared with traditional methods was credited to the creation of a shape-selective cavity that was a result of the hydrophilic structure of DES. The chitosan microspheres-magnetic graphene oxide imprinted by DES witnessed a high ability to adsorb chlorophenol compounds and their derivatives. Fig. 10 shows the preparation process of the molecularly imprinted chitosan microspheres in combination with DES (Li & Row, 2020).

4.3. DESs-chitosan combinations for producing beads and monoliths

Two types of DES, including ChCl-urea and ChCl–glycerol, were utilized to synthesize chitosan–DES beads to remove malachite green dye molecules from aqueous solutions. The mixture of chitosan (10 g) and DES (300 mL) was stirred at 60 °C for 1 h. The suspension of chitosan-DES mixture NaOH (0.5 M NaOH) results in chitosan beads. The resulting beads displayed a stable structure in the aqueous environment. The difference between chitosan-ChCl-urea and chitosan-ChCl-glycerol was in the OH stretching, which disclosed more shift for chitosan-ChCl-glycerol in comparison to chitosan–ChCl-urea, this was ascribed to the existence of a huge amount of OH in the glycerol constituent of chitosan-ChCl-glycerol. Notably, the higher number of OH groups means more and stronger electronegativity of atoms and bond length, which contribute to strong intermolecular interaction and thus a more robust hydrogen bond between DES and chitosan structure. Chitosan-ChCl-glycerol witnessed a rougher and more porous structure compared with chitosan-ChCl-urea, which caused more small openings and contact areas. In particular, the hydrolysis of the chitosan molecule chain upregulated the surface area of DESs-chitosan beads compared with pristine chitosan, showing pore sizes as 2 < diameter < 50 nm. The maximum adsorption capacity values of chitosan-ChCl-urea and chitosan-ChCl-glycerol were calculated as 6.54 mg/g and 8.64 mg/g, respectively, such values were higher than pure chitosan beads as a result of higher surface area and active sites (Sadiq, Rahim, & Suah, 2020). Fig. 11 displays the FTIR analysis of pure chitosan beads, chitosan-DES beads before and after malachite green dye adsorption. The FTIR analysis of chitosan-DES beads nearly remained unchanged compared to the pure chitosan beads as a result of a weak intermolecular interactions occurred in the DES functionalized chitosan beads.

Carbon aero- or xerogel monoliths can be applicable in several applications, including, catalyst support for electrochemical devices, water purification, and CO_2 capture. However, the employment of carbon monoliths has been restricted by the challenges in shaping and processing. The preparation process of carbon monoliths includes different stages containing the infiltration of monolithic templates, the carbonization of resins, and the activation of structured mesophase. The complex and additional synthetic stages, such as template elimination and activation process, and low environmentally friendly as a result of the existence of phenol-based compounds or formaldehyde, urged the invention of new eco-friendly approaches. Hence, DES-chitosan based structures can be operated to remove the aforementioned drawbacks, together with the increase in mesoporosity, nitrogen-content, and functionality of the prepared carbon monoliths compared with traditional techniques; also, this material provides more active sites for the adsorption of the different adsorbate. Towards the preparation of monolith, the mixture of hexaketocyclohexane-urea DES, chitosan, acetic acid and, water was autoclaved at 100 °C for 12 h. The prepared gel monolith was removed and rinsed with deionized water. After the drying process, the carbonization process was performed at 500 °C for 1 h (under nitrogen atmosphere). FTIR analysis revealed the disruption of the interconnection of hydrogen in the pristine chitosan, creating new hydrogen bonds between chitosan and DES structure in the monoliths. A huge amount of ketone- and hydroxy-functionalities in the DES structure increased the interaction between DES and chitosan structures by hydrogen bonding. After hydrothermal processing, covalent connections between these functionalities, and the amine- and amide-

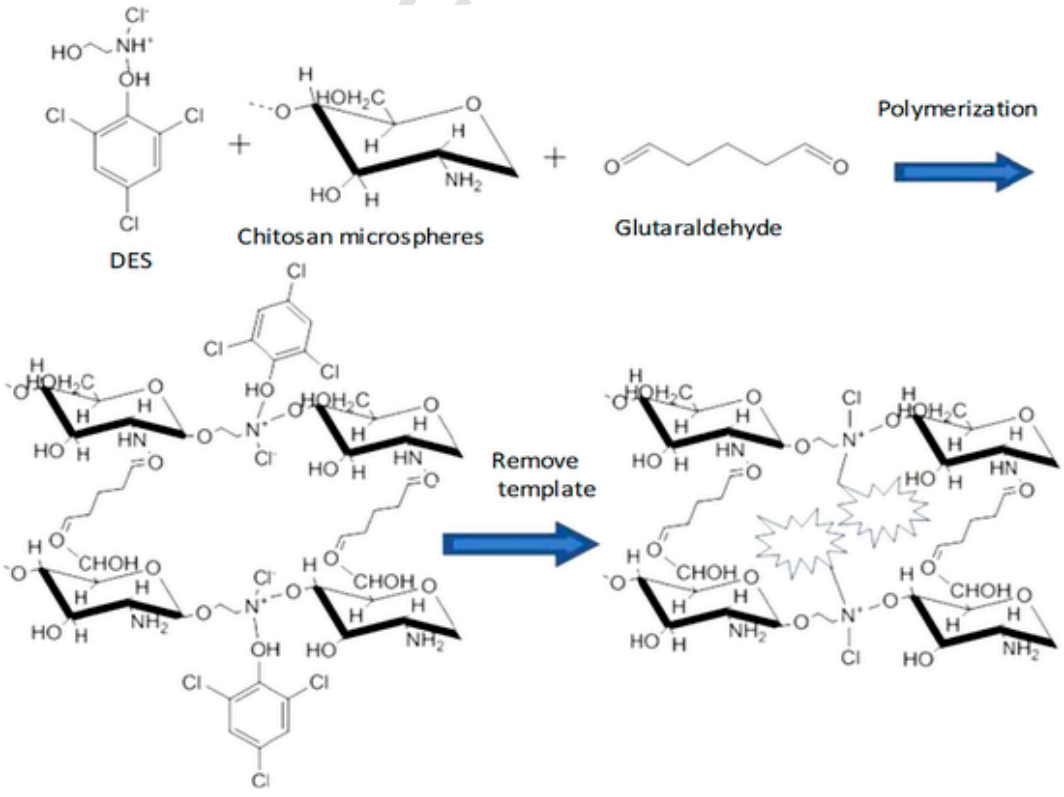

Fig. 10. The preparation process of the molecularly imprinted chitosan microspheres in combination with DES (Li & Row, 2020) (License 5140340775834).

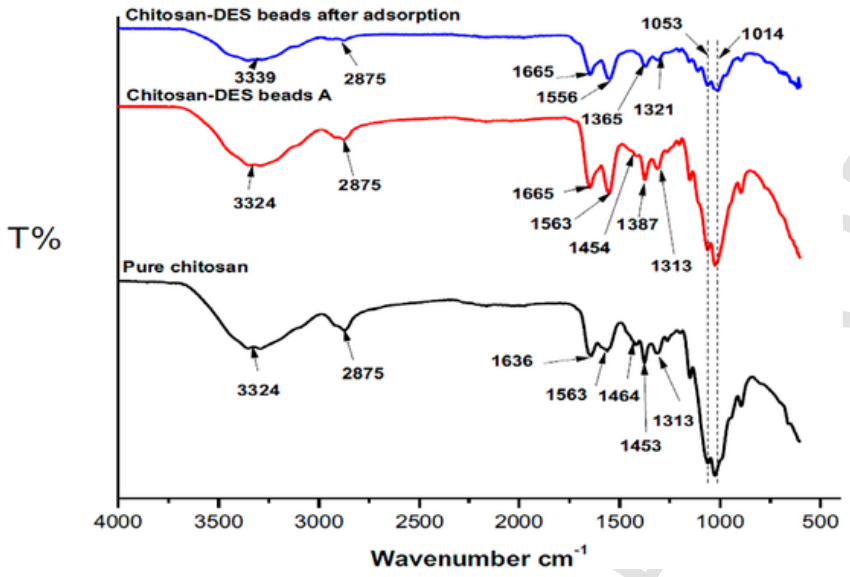

Fig. 11. FTIR analysis of pure chitosan beads, chitosan-DES beads before and after malachite green adsorption (Sadiq et al., 2020) (License 5140360101525). (For interpretation of the references to color in this figure legend, the reader is referred to the web version of this article.)

functionalities of the chitosan, caused a rigid polymer network of the DES-chitosan-based carbon monoliths. The transformation in the carbonization process, from the *net*-like structure of the precursor polymer to the morphology of interconnected primary nanospheres, was approved by SEM images. As part of the characterization, the surface area of the material was calculated about 348 m^2/g using BET analysis, which was more than only 78 m^2/g of the initial polymer monolith. This was attributed to the highly polymer-like structure of pristine monolith without DES that cannot endure crystallization forces within the drying process. The prepared monoliths displayed higher adsorption capacity (ca. 63 mg/g) compared with pristine monoliths for the adsorption of Rhodamine B dye, which was ascribed to the more surface area and functionality of prepared monoliths by DES (Jordan, Yu, Yu, Antonietti, & Fechler, 2018).

4.4. The use DES-chitosan based material as a support

The extraction of proteins and DNA has been studied considering DES as solvent out of the consideration of superior features compared to other solvents including, design ability and biocompatibility. To practicalize the use of DES, DES has been proposed as a modifier for support materials. As an example, chitosan-modified Fe_3O_4-magnetized multi-walled carbon nanotubes (mCS/MWCNTs) were coated on a polyethylene glycol-based DES to enhance the solid-phase extraction of salmon sperm DNA. Polyethylene glycol (as HBD) and tetraethylammonium chloride (as HBA) were selected to produce DES solvent. The mixture of CS/MWCNTs and DES was stirred and sonicated for 1 h. The resulting DES-CS/MWCNT was dried at 50 °C under vacuum. The electrostatic interaction was mentioned as the main interaction between DNA anion and the cation part of DES, which performed a vital part of the DNA extraction process. 143.5 mg/g was recorded for the DNA extraction using DES-CS/MWCNT, and the reusability of DES-CS/MWCNT was proved after three cycles. (Xu et al., 2017).

5. Conclusions and future perspectives

This review elucidated comprehensive evidence on the application of DES solvents in the sustainable extraction of chitin and its derivative chitosan structures. The advantages and disadvantages of DES-chitin and DES-chitosan structures were addressed to provide a better perspective for optimal utilization of DES in the chitin and chitosan structures, which may promote the industrialization of chitin constructions.

It is important to mention that the core application of DES in the chitin area has been directed to extract the biopolymer from different resources. The extracted chitin by DES presented a high purity (over 90%) and crystallinity (over 80%) depending on the type of DES used. To date, it is likely, ChCl-based DES (especially conformed to organic acids such as malic, lactic malonic acids) are among the most assayed green solvents for such a purpose, obtaining well-designed nanocrystal structure with different morphologies. Thanks to the selective interaction between DES and the raw material of chitin, the resulting product presents an excellent dissolution degree of chitin with high purity. Also, the compatibility between DES and chitin source leads chitin to preserve its crystallinity at the end of the extraction process. Over the course of this review, it has been pointed out that the kind of HBA and HBD (along with their mole ratio), the ratio between DES and raw material of chitin and extraction method can affect the quality of produced chitin, however, by handling such operating parameters during extraction, the resulting chitin can be precisely tuned to meet the desired physiochemical parameters towards specific applications. For instance, it has been evidenced that chitin extraction by ChCl-urea promoted a γ-mono-phase in the tailored films.

On the other hand, the main application of DES in the chitosan structure has been focused to increase the plasticity and mechanical properties (e.g., elongation at break) of the resulting DES-chitosan films. DES can greatly improve the flexibility and resistivity against fracture of chitosan films, compared with other solvents. Moreover, by optimizing DES-chitosan structure, it can be utilized in the food packaging industry and membrane technologies, which may result in new materials with high adsorption capacity out of consideration of the high functionality of the chitosan structure. Finally, considering that plenty of DESs can be formed based on different HBA and HBD molecules, the types of compounds and their molar ratio will be determinants for the final properties of the new sustainable chitosan structure. At this point, it is quite possible that new DESs will be synthesized according to their potentiality and inherent features in comparison to traditional solvents, therefore, such new DESs could be applied in tailoring new sustainable biopolymer-based structure contributing to the new era of "green chemistry".

Acknowledgment

Grzegorz Boczkaj gratefully acknowledge the financial support from the National Science Centre, Warsaw, Poland – decision no. UMO-

2018/30/E/ST8/00642. R. Castro-Muñoz acknowledges the financial support from Polish National Agency for Academic Exchange (NAWA) under Ulam Programme (Agreement No. PPN/ULM/2020/1/00005/U/00001). V. Vatanpour acknowledges the financial support of the Kharazmi University (Iran) from Kharazmi membrane research core (Grant number: H/4/360).

References

Akyuz, L., Kaya, M., Koc, B., Mujtaba, M., Ilk, S., Labidi, J., … Yildiz, A. (2017). *Diatomite as a novel composite ingredient for chitosan film with enhanced physicochemical properties. International Journal of Biological Macromolecules*, *105*, 1401–1411. https://doi.org/10.1016/j.ijbiomac.2017.08.161.

Alishahi, A., & Aïder, M. (2012). *Applications of chitosan in the seafood industry and aquaculture: A review. Food and Bioprocess Technology*, *5*(3), 817–830. https://doi.org/10.1007/s11947-011-0664-x.

Almeida, C. M. R., Magalhães, J. M. C. S., Souza, H. K. S., & Gonçalves, M. P. (2018). *The role of choline chloride-based deep eutectic solvent and curcumin on chitosan films properties. Food Hydrocolloids*, *81*, 456–466. https://doi.org/10.1016/j.foodhyd.2018.03.025.

Bakshi, P. S., Selvakumar, D., Kadirvelu, K., & Kumar, N. S. (2020). *Chitosan as an environment friendly biomaterial — A review on recent modifications and applications. International Journal of Biological Macromolecules*, *150*, 1072–1083. https://doi.org/10.1016/j.ijbiomac.2019.10.113.

Bangde, P. S., Jain, R., & Dandekar, P. (2016). *Alternative approach to synthesize methylated chitosan using deep eutectic solvents, biocatalyst and "green" methylating agents. ACS Sustainable Chemistry and Engineering*, *4*(6), 3552–3557. https://doi.org/10.1021/acssuschemeng.6b00653.

Campos, C. A., Gerschenson, L. N., & Flores, S. K. (2011). *Development of edible films and coatings with antimicrobial activity. Food and Bioprocess Technology*, *4*(6), 849–875. https://doi.org/10.1007/s11947-010-0434-1.

Castro-Muñoz, R. (2020). *Breakthroughs on tailoring pervaporation membranes for water desalination: A review. Water Research*, *187*. https://doi.org/10.1016/j.watres.2020.116428.

Castro-Muñoz, R., & Boczkaj, G. (2021). *Pervaporation zeolite-based composite membranes for solvent separations. Molecules*, *26*, 1242.

Castro-Muñoz, R., Buera-Gonzalez, J., de la Iglesia, O., Galiano, F., Fíla, V., Malankowska, M., Rubio, C., Figoli, A., Tellez, C., & Coronas, J. (2019). Towards the dehydration of ethanol using pervaporation cross-linked poly(vinyl alcohol)/graphene oxide membranes. Journal of Membrane Science, 582, 423–434. doi:doi:https://doi.org/10.1016/j.memsci.2019.03.076.

Castro-Muñoz, R., Galiano, F., & Figoli, A. (2020). *Recent advances in pervaporation hollow fiber membranes for dehydration of organics. Chemical Engineering Research and Design*, *164*. https://doi.org/10.1016/j.cherd.2020.09.028.

Castro-Muñoz, R., Gontarek, E., & Figoli, A. (2019). Membranes for toxic- and heavy-metal removal. *Current trends and future developments on (bio-)membranes: Membranes in environmental applications*. https://doi.org/10.1016/B978-0-12-816778-6.00007-2.

Castro-Muñoz, R., Gonzalez-Melgoza, L., & Garcia-Depraect, O. (2021). *Ongoing progress on novel nanocomposite membranes for the separation of heavy metals from contaminated water. Chemosphere*, *270*, 129421. https://doi.org/10.1016/j.chemosphere.2020.129421.

Castro-Muñoz, R., & González-Valdez, J. (2019). *New trends in biopolymer-based membranes for pervaporation. Molecules*, *24*(19). https://doi.org/10.3390/molecules24193584.

Castro-Muñoz, R., Gonzalez-Valdez, J., & Ahmad, Z. (2020). *High-performance pervaporation chitosan-based membranes: New insights and perspectives. Reviews in Chemical Engineering*, 1–16. https://doi.org/10.1515/revce-2019-0051.

Castro-Muñoz, R., Agrawal, K. V., & Coronas, J. (2020). *Ultrathin permselective membranes: The latent way for efficient gas separation. RSC Advances*, *10*(21), 12653–12670. https://doi.org/10.1039/d0ra02254c.

Delgado-Rangel, L. H., Huerta-Saquero, A., Eufracio-García, N., Meza-Villezcas, A., Mota-Morales, J. D., & González-Campos, J. B. (2020). *Deep eutectic solvent-assisted phase separation in chitosan solutions for the production of 3D monoliths and films with tailored porosities. International Journal of Biological Macromolecules*, *164*, 4084–4094. https://doi.org/10.1016/j.ijbiomac.2020.08.254.

Díaz-Montes, E., & Castro-Muñoz, R. (2021a). *Edible films and coatings as food-quality preservers: An overview. Foods*, *10*(2), 249. https://doi.org/10.3390/foods10020249.

Díaz-Montes, E., & Castro-Muñoz, R. (2021b). *Trends in chitosan as a primary biopolymer for functional films and coatings manufacture for food and natural products. Polymers*, *13*(5), 1–28. https://doi.org/10.3390/polym13050767.

Duan, B., Chang, C., Ding, B., Cai, J., Xu, M., Feng, S., … Zhang, L. (2013). *High strength films with gas-barrier fabricated from chitin solution dissolved at low temperature. Journal of Materials Chemistry A*, *1*(5), 1867–1874. https://doi.org/10.1039/c2ta00068g.

Fan, Y., Saito, T., & Isogai, A. (2008). *Chitin nanocrystals prepared by TEMPO-mediated oxidation of α-chitin. Biomacromolecules*, *9*(1), 192–198. https://doi.org/10.1021/bm700966g.

Feng, M., Lu, X., Zhang, J., Li, Y., Shi, C., Lu, L., & Zhang, S. (2019). *Direct conversion of shrimp shells to: O-acylated chitin with antibacterial and anti-tumor effects by natural deep eutectic solvents. Green Chemistry*, *21*(1), 87–98. https://doi.org/10.1039/c8gc02506a.

Francisco, M., Van Den Bruinhorst, A., & Kroon, M. C. (2012). *New natural and renewable low transition temperature mixtures (LTTMs): Screening as solvents for lignocellulosic biomass processing. Green Chemistry*, *14*(8), 2153–2157. https://doi.org/10.1039/c2gc35660k.

Galvis-Sánchez, A. C., Castro, M. C. R., Biernacki, K., Gonçalves, M. P., & Souza, H. K. S. (2018). *Natural deep eutectic solvents as green plasticizers for chitosan thermoplastic production with controlled/desired mechanical and barrier properties. Food Hydrocolloids*, *82*, 478–489. https://doi.org/10.1016/j.foodhyd.2018.04.026.

Galvis-Sánchez, A. C., Sousa, A. M. M., Hilliou, L., Gonçalves, M. P., & Souza, H. K. S. (2016). *Thermo-compression molding of chitosan with a deep eutectic mixture for biofilms development. Green Chemistry*, *18*(6), 1571–1580. https://doi.org/10.1039/c5gc02231b.

Guerrero, P., Muxika, A., Zarandona, I., & de la Caba, K. (2019). *Crosslinking of chitosan films processed by compression molding. Carbohydrate Polymers*, *206*, 820–826. https://doi.org/10.1016/j.carbpol.2018.11.064.

Haghighi, H., Licciardello, F., Fava, P., Siesler, H. W., & Pulvirenti, A. (2020). *Recent advances on chitosan-based films for sustainable food packaging applications. Food Packaging and Shelf Life*, *26*(July), 100551. https://doi.org/10.1016/j.fpsl.2020.100551.

Hajji, S., Ghorbel-Bellaaj, O., Younes, I., Jellouli, K., & Nasri, M. (2015). *Chitin extraction from crab shells by Bacillus bacteria. Biological activities of fermented crab supernatants. International Journal of Biological Macromolecules*, *79*, 167–173. https://doi.org/10.1016/j.ijbiomac.2015.04.027.

Hamed, I., Özogul, F., & Regenstein, J. M. (2016). *Industrial applications of crustacean by-products (chitin, chitosan, and chitooligosaccharides): A review. Trends in Food Science and Technology*, *48*, 40–50. https://doi.org/10.1016/j.tifs.2015.11.007.

Hong, S., Yang, Q., Yuan, Y., Chen, L., Song, Y., & Lian, H. (2019). *Sustainable co-solvent induced one step extraction of low molecular weight chitin with high purity from raw lobster shell. Carbohydrate Polymers*, *205*, 236–243. https://doi.org/10.1016/j.carbpol.2018.10.045.

Hong, S., Yuan, Y., Yang, Q., Chen, L., Deng, J., Chen, W., … Liimatainen, H. (2019). *Choline chloride-zinc chloride deep eutectic solvent mediated preparation of partial O-acetylation of chitin nanocrystal in one step reaction. Carbohydrate Polymers*, *220*(March), 211–218. https://doi.org/10.1016/j.carbpol.2019.05.075.

Hong, S., Yuan, Y., Yang, Q., Zhu, P., & Lian, H. (2018). *Versatile acid base sustainable solvent for fast extraction of various molecular weight chitin from lobster shell. Carbohydrate Polymers*, *201*, 211–217. https://doi.org/10.1016/j.carbpol.2018.08.059.

Hong, S., Yuan, Y., Zhang, K., Lian, H., & Liimatainen, H. (2020). *Efficient hydrolysis of chitin in a deep eutectic solvent synergism for production of chitin nanocrystals. Nanomaterials*, *10*(5). https://doi.org/10.3390/nano10050869.

Hosseini, S. F., & Gómez-Guillén, M. C. (2018). *A state-of-the-art review on the elaboration of fish gelatin as bioactive packaging: Special emphasis on nanotechnology-based approaches. Trends in Food Science and Technology*, *79*, 125–135. https://doi.org/10.1016/j.tifs.2018.07.022.

Huang, W. C., Zhao, D., Guo, N., Xue, C., & Mao, X. (2018). *Green and facile production of chitin from crustacean shells using a natural deep eutectic solvent. Journal of Agricultural and Food Chemistry*, *66*(45), 11897–11901. https://doi.org/10.1021/acs.jafc.8b03847.

Huet, G., Hadad, C., Husson, E., Laclef, S., Lambertyn, V., Araya Farias, M., … Van Nhien, A. N. (2020). *Straightforward extraction and selective bioconversion of high purity chitin from Bombyx eri larva: Toward an integrated insect biorefinery. Carbohydrate Polymers*, *228* (August 2019), 115382. https://doi.org/10.1016/j.carbpol.2019.115382.

Jakubowska, E., Gierszewska, M., Nowaczyk, J., & Olewnik-Kruszkowska, E. (2020). *Physicochemical and storage properties of chitosan-based films plasticized with deep eutectic solvent. Food Hydrocolloids*, *108*(January), 106007. https://doi.org/10.1016/j.foodhyd.2020.106007.

Jakubowska, E., Gierszewska, M., Nowaczyk, J., & Olewnik-Kruszkowska, E. (2021). *The role of a deep eutectic solvent in changes of physicochemical and antioxidative properties of chitosan-based films. Carbohydrate Polymers*, *255*(July 2020), 117527. https://doi.org/10.1016/j.carbpol.2020.117527.

Janicka, P., Przyjazny, A., & Boczkaj, G. (2021). *Novel "acid-tuned" deep eutectic solvents based on protonated L-proline. Journal of Molecular Liquids*, 115965. https://doi.org/10.1016/j.molliq.2021.115965.

Jiang, W. H., Gu, W. M., Xiong, M. J., He, K. P., Xu, X. Y., Zhang, W. X., … Cao, S. L. (2020). *Commentary: Preparation, characterization and application of rod-like chitin nanocrystal by using p-toluenesulfonic acid/choline chloride deep eutectic solvent as a hydrolytic media. Frontiers in Bioengineering and Biotechnology*, *8*(February), 304–310. https://doi.org/10.3389/fbioe.2020.00505.

Jordan, T., Yu, Z. L., Yu, S. H., Antonietti, M., & Fechler, N. (2018). *Porous nitrogen-doped carbon monoliths derived from biopolymer-structured liquid precursors. Microporous and Mesoporous Materials*, *255*, 53–60. https://doi.org/10.1016/j.micromeso.2017.07.032.

Joseph, S. M., Krishnamoorthy, S., Paranthaman, R., Moses, J. A., & Anandharamakrishnan, C. (2021). *A review on source-specific chemistry, functionality, and applications of chitin and chitosan. Carbohydrate Polymer Technologies and Applications*, *2* (December), 100036. https://doi.org/10.1016/j.carpta.2021.100036.

Kadokawa, J. I., Setoguchi, T., & Yamamoto, K. (2013). *Preparation of highly flexible chitin nanofiber-graft-poly(γ-L-glutamic acid) network film. Polymer Bulletin*, *70*(12), 3279–3289. https://doi.org/10.1007/s00289-013-1020-2.

Kalaycıoğlu, Z., Torlak, E., Akın-Evingür, G., Özen, İ., & Erim, F. B. (2017). *Antimicrobial and physical properties of chitosan films incorporated with turmeric extract. International Journal of Biological Macromolecules*, *101*, 882–888. https://doi.org/10.1016/j.ijbiomac.2017.03.174.

Khajavian, M., Salehi, E., & Vatanpour, V. (2020a). *Chitosan/polyvinyl alcohol thin membrane adsorbents modified with zeolitic imidazolate framework (ZIF-8) nanostructures: Batch adsorption and optimization. Separation and Purification Technology*, *241*. https://doi.org/10.1016/j.seppur.2020.116759.

Khajavian, M., Salehi, E., & Vatanpour, V. (2020b). *Nano filtration of dye solution using chitosan/poly(vinyl alcohol)/ZIF-8 thin film composite adsorptive membranes with PVDF membrane beneath as support. Carbohydrate Polymers*, *247*(June), 116693. https://doi.org/10.1016/j.carbpol.2020.116693.

Khayrova, A., Lopatin, S., & Varlamov, V. (2021). *Obtaining chitin, chitosan and their melanin complexes from insects. International Journal of Biological Macromolecules*, *167* (xxxx), 1319–1328. https://doi.org/10.1016/j.ijbiomac.2020.11.086.

Kumar, A. K., Sharma, S., Dixit, G., Shah, E., Patel, A., & Boczkaj, G. (2020). *Techno-economic evaluation of a natural deep eutectic solvent-based biorefinery: Exploring different design scenarios. Biofuels, Bioproducts and Biorefining*, *14*(4), 746–763. https://doi.org/

10.1002/bbb.2110.
Lasheen, M. R., El-Sherif, I. Y., Tawfik, M. E., El-Wakeel, S. T., & El-Shahat, M. F. (2016). *Preparation and adsorption properties of nano magnetite chitosan films for heavy metal ions from aqueous solution*. *Materials Research Bulletin*, *80*, 344–350. https://doi.org/10.1016/j.materresbull.2016.04.011.
Lasheen, M. R., El-Sherif, I. Y., Tawfik, M. E., El-Wakeel, S. T., El-Shahat, M. F., Joseph, S. M., … Singh, S. K. (2019). *Engineering strategies for chitin nanofibers*. *International Journal of Biological Macromolecules*, *5*(September 2020), 820–826. https://doi.org/10.1016/j.ijbiomac.2018.10.109.
Li, G., & Row, K. H. (2020). *Deep eutectic solvents skeleton typed molecularly imprinted chitosan microsphere coated magnetic graphene oxide for solid-phase microextraction of chlorophenols from environmental water*. *Journal of Separation Science*, *43*(6), 1063–1070. https://doi.org/10.1002/jssc.201901159.
Li, W. H., Qin, F., & Zhao, Y. Y. (2020). *A note on uninorms with continuous underlying operators*. *Fuzzy Sets and Systems*, *386*, 36–47. https://doi.org/10.1016/j.fss.2019.03.007.
Liao, J., & Huang, H. (2020). *A fungal chitin derived from Hericium erinaceus residue: Dissolution, gelation and characterization*. *International Journal of Biological Macromolecules*, *152*, 456–464. https://doi.org/10.1016/j.ijbiomac.2020.02.309.
Ma, Q., Gao, X., Bi, X., Han, Q., Tu, L., Yang, Y., … Wang, M. (2020). *Dissolution and deacetylation of chitin in ionic liquid tetrabutylammonium hydroxide and its cascade reaction in enzyme treatment for chitin recycling*. *Carbohydrate Polymers*, *230*, 115605. https://doi.org/10.1016/j.carbpol.2019.115605.
Ma, W., Dai, Y., & Row, K. H. (2018). *Molecular imprinted polymers based on magnetic chitosan with different deep eutectic solvent monomers for the selective separation of catechins in black tea*. *Electrophoresis*, *39*(15), 2039–2046. https://doi.org/10.1002/elps.201800034.
Mahajan, T., Bangde, P., Dandekar, P., & Jain, R. (2020). *Greener approach for synthesis of N,N,N-trimethyl chitosan (TMC) using ternary deep eutectic solvents (TDESs)*. *Carbohydrate Research*, *493*, 108033. https://doi.org/10.1016/j.carres.2020.108033.
Makoś, P., & Boczkaj, G. (2019). *Deep eutectic solvents based highly efficient extractive desulfurization of fuels — Eco-friendly approach*. *Journal of Molecular Liquids*, *296*, 111916. https://doi.org/10.1016/j.molliq.2019.111916.
Makoś, P., Fernandes, A., Przyjazny, A., & Boczkaj, G. (2018). *Sample preparation procedure using extraction and derivatization of carboxylic acids from aqueous samples by means of deep eutectic solvents for gas chromatographic-mass spectrometric analysis*. *Journal of Chromatography A*, *1555*, 10–19. https://doi.org/10.1016/j.chroma.2018.04.054.
Martins, J. T., Cerqueira, M. A., & Vicente, A. A. (2012). *Influence of α-tocopherol on physicochemical properties of chitosan-based films*. *Food Hydrocolloids*, *27*(1), 220–227. https://doi.org/10.1016/j.foodhyd.2011.06.011.
Mohan, K., Ganesan, A. R., Muralisankar, T., Jayakumar, R., Sathishkumar, P., Uthayakumar, V., … Revathi, N. (2020). *Recent insights into the extraction, characterization, and bioactivities of chitin and chitosan from insects*. *Trends in Food Science and Technology*, *105*(May), 17–42. https://doi.org/10.1016/j.tifs.2020.08.016.
Montalvo, C., López Malo, A., & Palou, E. (2012). *Películas comestibles de proteína: características, propiedades y aplicaciones*. *Temas Selectos de Ingeniería de Alimentos*, *2*, 32–46. https://doi.org/10.1016/j.jcis.2012.04.042.
Mujtaba, M., Morsi, R. E., Kerch, G., Elsabee, M. Z., Kaya, M., Labidi, J., & Khawar, K. M. (2019). *Current advancements in chitosan-based film production for food technology; a review*. *International Journal of Biological Macromolecules*, *121*, 889–904. https://doi.org/10.1016/j.ijbiomac.2018.10.109.
Mukesh, C., Mondal, D., Sharma, M., & Prasad, K. (2014). *Choline chloride-thiourea, a deep eutectic solvent for the production of chitin nanofibers*. *Carbohydrate Polymers*, *103*(1), 466–471. https://doi.org/10.1016/j.carbpol.2013.12.082.
Mukesh, C., Mondal, D., Sharma, M., Prasad, K., Yuan, Y., Hong, S., … Lian, H. (2019). *One-pot production of chitin with high purity from lobster shells using choline chloride–malonic acid deep eutectic solvent*. *Carbohydrate Polymers*, *177*(1), 466–471. https://doi.org/10.1039/c3ra43404d.
Musarurwa, H., & Tavengwa, N. T. (2021). *Deep eutectic solvent-based dispersive liquid-liquid micro-extraction of pesticides in food samples*. *Food Chemistry*, *342*, 127943. https://doi.org/10.1016/j.foodchem.2020.127943.
Naghibi, S. A., Salehi, E., Khajavian, M., Vatanpour, V., & Sillanpää, M. (2021). *Multivariate data-based optimization of membrane adsorption process for wastewater treatment: Multi-layer perceptron adaptive neural network versus adaptive neural fuzzy inference system*. *Chemosphere*, *267*. https://doi.org/10.1016/j.chemosphere.2020.129268.
Özel, N., & Elibol, M. (2021). *A review on the potential uses of deep eutectic solvents in chitin and chitosan related processes*. *Carbohydrate Polymers*, *262*, 117942. https://doi.org/https://.org/10.1016/j.carbpol.2021.117942.
Pădureţu, C. C., Apetroaei, M. R., Rău, I., & Schroder, V. (2018). *Characterization of chitosan extracted from different Romanian Black Sea crustaceans*. *UPB Scientific Bulletin, Series B: Chemistry and Materials Science*, *80*(3), 13–24.
Panwar, R., Raghuwanshi, N., Srivastava, A. K., Sharma, A. K., & Pruthi, V. (2018). *In-vivo sustained release of nanoencapsulated ferulic acid and its impact in induced diabetes*. *Materials Science and Engineering C*, *92*(August 2017), 381–392. https://doi.org/10.1016/j.msec.2018.06.055.
Pereira, P. F., & Andrade, C. T. (2017). *Optimized pH-responsive film based on a eutectic mixture-plasticized chitosan*. *Carbohydrate Polymers*, *165*, 238–246. https://doi.org/10.1016/j.carbpol.2017.02.047.
Pérez-Guzmán, C. J., & Castro-Muñoz, R. (2020). *A review of zein as a potential biopolymer for tissue engineering and nanotechnological applications*. *Processes*, *8*(11). https://doi.org/10.3390/pr8111376.
Pillai, C. K. S., Paul, W., & Sharma, C. P. (2009). *Chitin and chitosan polymers: Chemistry, solubility and fiber formation*. *Progress in Polymer Science (Oxford)*, *34*(7), 641–678. https://doi.org/10.1016/j.progpolymsci.2009.04.001.
Qiao, C., Ma, X., Zhang, J., & Yao, J. (2017). *Molecular interactions in gelatin/chitosan composite films*. *Food Chemistry*, *235*, 45–50. https://doi.org/10.1016/j.foodchem.2017.05.045.
Ramírez-Wong, D. G., Ramírez-Cardona, M., Sánchez-Leija, R. J., Rugerio, A., Mauricio-Sánchez, R. A., Hernández-Landaverde, M. A., … Luna-Bárcenas, G. (2016). *Sustainable-solvent-induced polymorphism in chitin films*. *Green Chemistry*, *18*(15), 4303–4311. https://doi.org/10.1039/c6gc00628k.
Sadiq, A. C., Rahim, N. Y., & Suah, F. B. M. (2020). *Adsorption and desorption of malachite green by using chitosan-deep eutectic solvents beads*. *International Journal of Biological Macromolecules*, *164*, 3965–3973. https://doi.org/10.1016/j.ijbiomac.2020.09.029.
Salehi, E., Madaeni, S. S., Rajabi, L., Derakhshan, A. A., Daraei, S., & Vatanpour, V. (2013). *Static and dynamic adsorption of copper ions on chitosan/polyvinyl alcohol thin adsorptive membranes: Combined effect of polyethylene glycol and aminated multi-walled carbon nanotubes*. *Chemical Engineering Journal*, *215–216*, 791–801. https://doi.org/10.1016/j.cej.2012.11.071.
Salehi, E., Madaeni, S. S., Rajabi, L., Vatanpour, V., Derakhshan, A. A., Zinadini, S., … Ahmadi Monfared, H. (2012). *Novel chitosan/poly(vinyl) alcohol thin adsorptive membranes modified with amino functionalized multi-walled carbon nanotubes for Cu(II) removal from water: Preparation, characterization, adsorption kinetics and thermodynamics*. *Separation and Purification Technology*, *89*, 309–319. https://doi.org/10.1016/j.seppur.2012.02.002.
Saravana, P. S., Ho, T. C., Chae, S. J., Cho, Y. J., Park, J. S., Lee, H. J., & Chun, B. S. (2018). *Deep eutectic solvent-based extraction and fabrication of chitin films from crustacean waste*. *Carbohydrate Polymers*, *195*(April), 622–630. https://doi.org/10.1016/j.carbpol.2018.05.018.
Sarmad, S., Xie, Y., Mikkola, J. P., & Ji, X. (2016). *Screening of deep eutectic solvents (DESs) as green CO_2 sorbents: From solubility to viscosity*. *New Journal of Chemistry*, *41*(1), 290–301. https://doi.org/10.1039/c6nj03140d.
Sharma, B., Sharma, S., & Jain, P. (2021). *Leveraging advances in chemistry to design biodegradable polymeric implants using chitosan and other biomaterials*. *International Journal of Biological Macromolecules*, *169*, 414–427. https://doi.org/10.1016/j.ijbiomac.2020.12.112.
Sharma, M., Mukesh, C., Mondal, D., & Prasad, K. (2013). *Dissolution of α-chitin in deep eutectic solvents*. *RSC Advances*, *3*(39), 18149–18155. https://doi.org/10.1039/c3ra43404d.
Singh, S. K. (2019). *Solubility of lignin and chitin in ionic liquids and their biomedical applications*. *International Journal of Biological Macromolecules*, *132*, 265–277. https://doi.org/10.1016/j.ijbiomac.2019.03.182.
Smirnov, M. A., Sokolova, M. P., Tolmachev, D. A., Vorobiov, V. K., Kasatkin, I. A., Smirnov, N. N., … Yakimansky, A. V. (2020). *Green method for preparation of cellulose nanocrystals using deep eutectic solvent*. *Cellulose*, *27*(8), 4305–4317. https://doi.org/10.1007/s10570-020-03100-1.
Smith, E. L., Abbott, A. P., & Ryder, K. S. (2014). *Deep eutectic solvents (DESs) and their applications*. *Chemical Reviews*, *114*(21), 11060–11082. https://doi.org/10.1021/cr300162p.
Taghizadeh, M., Taghizadeh, A., Vatanpour, V., Ganjali, M. R., & Saeb, M. R. (2021). *Deep eutectic solvents in membrane science and technology: Fundamental, preparation, application, and future perspective*. *Separation and Purification Technology*, *258*, 118015. https://doi.org/10.1016/j.seppur.2020.118015.
Tan, Y. N., Lee, P. P., & Chen, W. N. (2020). *Microbial extraction of chitin from seafood waste using sugars derived from fruit waste-stream*. *AMB Express*, *10*(1). https://doi.org/10.1186/s13568-020-0954-7.
Trung, T. S., Tram, L. H., Van Tan, N., Van Hoa, N., Minh, N. C., Loc, P. T., & Stevens, W. F. (2020). *Improved method for production of chitin and chitosan from shrimp shells*. *Carbohydrate Research*, *489*, 107913. https://doi.org/10.1016/j.carres.2020.107913.
Tsurkan, M. V., Voronkina, A., Khrunyk, Y., Wysokowski, M., Petrenko, I., & Ehrlich, H. (2021). *Progress in chitin analytics*. *Carbohydrate Polymers*, *252*, 117204. https://doi.org/10.1016/j.carbpol.2020.117204.
Ul, H., Balal, M., Castro-Muñoz, R., Hussain, Z., Sa, F., Ullah, S., & Boczkaj, G. (2021). *Deep eutectic solvents based assay for extraction and determination of zinc in fish and eel samples using FAAS*. *333*, 1–5. https://doi.org/10.1016/j.molliq.2021.115930.
Ursino, C., Castro-Muñoz, R., Drioli, E., Gzara, L., Albeirutty, M. H., & Figoli, A. (2018). *Progress of nanocomposite membranes for water treatment*. *Membranes*, *8*(2). https://doi.org/10.3390/membranes8020018.
Van Hoa, N., Vuong, N. T. H., Minh, N. C., Cuong, H. N., & Trung, T. S. (2020). *Squid pen chitosan nanoparticles: Small size and high antibacterial activity*. *Polymer Bulletin*, 0123456789. https://doi.org/10.1007/s00289-020-03488-7.
Vatanpour, V., Dehqan, A., & Harifi-Mood, A. R. (2020). *Ethaline deep eutectic solvent as a hydrophilic additive in modification of polyethersulfone membrane for antifouling and separation improvement*. *Journal of Membrane Science*, *614*, 118528.
Vatanpour, V., Salehi, E., Sahebjamee, N., & Ashrafi, M. (2018). *Novel chitosan/polyvinyl alcohol thin membrane adsorbents modified with detonation nanodiamonds: Preparation, characterization, and adsorption performance*. *Arabian Journal of Chemistry.*. https://doi.org/10.1016/j.arabjc.2018.01.010.
Vicente, F. A., Bradić, B., Novak, U., & Likozar, B. (2020). *α-Chitin dissolution, N-deacetylation and valorization in deep eutectic solvents*. *Biopolymers*, *111*(5). https://doi.org/10.1002/bip.23351.
Vicente, F. A., Huš, M., Likozar, B., & Novak, U. (2021). *Chitin deacetylation using deep eutectic solvents: Ab initio-supported process optimization*. *ACS Sustainable Chemistry and Engineering*, *9*(10), 3874–3886. https://doi.org/10.1021/acssuschemeng.0c08976.
Vorobiov, V. K., Smirnov, M. A., Bobrova, N. V., & Sokolova, M. P. (2021). *Chitosan-supported deep eutectic solvent as bio-based electrolyte for flexible supercapacitor*. *Materials Letters*, *283*, 128889. https://doi.org/10.1016/j.matlet.2020.128889.
Wang, H., Rehman, K.u., Feng, W., Yang, D., Rehman, R.u., Cai, M., … Zheng, L. (2020). *Physicochemical structure of chitin in the developing stages of black soldier fly*. *International Journal of Biological Macromolecules*, *149*, 901–907. https://doi.org/10.1016/j.ijbiomac.2020.01.293.

Weaver, K. D., Kim, H. J., Sun, J., MacFarlane, D. R., & Elliott, G. D. (2010). *Cyto-toxicity and biocompatibility of a family of choline phosphate ionic liquids designed for pharmaceutical applications*. *Green Chemistry*, *12*(3), 507–551. https://doi.org/10.1039/b918726j.

Wong, C. Y., Wong, W. Y., Walvekar, R., Loh, K. S., Khalid, M., & Lim, K. L. (2018a). *Effect of deep eutectic solvent in proton conduction and thermal behaviour of chitosan-based membrane*. *Journal of Molecular Liquids*, *269*, 675–683. https://doi.org/10.1016/j.molliq.2018.08.102.

Wong, C. Y., Wong, W. Y., Walvekar, R., Loh, K. S., Khalid, M., & Lim, K. L. (2018b). *file:///D:/Prof. GB/Proposal/Rev 01/papers/chitosan and DES/Optimized pH-responsive film based on a eutectic.pdf*. *Journal of Molecular Liquids*, *269*, 675–683. https://doi.org/10.1016/j.molliq.2018.08.102.

Wong, W. Y., Wong, C. Y., Rashmi, W., & Khalid, M. (2018). *Choline chloride: Urea-based deep eutectic solvent as additive to proton conducting chitosan films*. *Journal of Engineering Science and Technology*, *13*(9), 2995–3006.

Xu, K., Wang, Y., Zhang, H., Yang, Q., Wei, X., Xu, P., & Zhou, Y. (2017). *Solid-phase extraction of DNA by using a composite prepared from multiwalled carbon nanotubes, chitosan, Fe_3O_4 and a poly(ethylene glycol)-based deep eutectic solvent*. *Microchimica Acta*, *184*(10), 4133–4140. https://doi.org/10.1007/s00604-017-2444-4.

Yavir, K., Konieczna, K., Marcinkowski, Ł., & Kloskowski, A. (2020). *Ionic liquids in the microextraction techniques: The influence of ILs structure and properties*. *TrAC — Trends in Analytical Chemistry*, *130*, 115994. https://doi.org/10.1016/j.trac.2020.115994.

Yuan, Y., Hong, S., Lian, H., Zhang, K., & Liimatainen, H. (2020). *Comparison of acidic deep eutectic solvents in production of chitin nanocrystals*. *Carbohydrate Polymers*, *236*(January). https://doi.org/10.1016/j.carbpol.2020.116095.

Zhang, Q., De Oliveira Vigier, K., Royer, S., & Jérôme, F. (2012). *Deep eutectic solvents: Syntheses, properties and applications*. *Chemical Society Reviews*, *41*(21), 7108–7146. https://doi.org/10.1039/c2cs35178a.

Zhao, D., Huang, W. C., Guo, N., Zhang, S., Xue, C., & Mao, X. (2019). *Two-step separation of chitin from shrimp shells using citric acid and deep eutectic solvents with the assistance of microwave*. *Polymers*, *11*(3). https://doi.org/10.3390/polym11030409.

Zhao, Y., Zhu, L., Li, W., Liu, J., Liu, X., & Huang, K. (2019). *Insights into enhanced adsorptive removal of rhodamine B by different chemically modified garlic peels: Comparison, kinetics, isotherms, thermodynamics and mechanism*. *Journal of Molecular Liquids*, *293*, 111516. https://doi.org/10.1016/j.molliq.2019.111516.

Zhou, P., Li, J., Yan, T., Wang, X., Huang, J., Kuang, Z., … Pan, M. (2019). *Selectivity of deproteinization and demineralization using natural deep eutectic solvents for production of insect chitin (Hermetia illucens)*. *Carbohydrate Polymers*, *225*(August). https://doi.org/10.1016/j.carbpol.2019.115255.

Zhu, P., Gu, Z., Hong, S., & Lian, H. (2017). *One-pot production of chitin with high purity from lobster shells using choline chloride–malonic acid deep eutectic solvent*. *Carbohydrate Polymers*, *177*(September), 217–223. https://doi.org/10.1016/j.carbpol.2017.09.001.

Zinadini, S., Zinatizadeh, A. A., Rahimi, M., Vatanpour, V., Zangeneh, H., & Beygzadeh, M. (2014). *Novel high flux antifouling nanofiltration membranes for dye removal containing carboxymethyl chitosan coated Fe_3O_4 nanoparticles*. *Desalination*, *349*, 145–154. https://doi.org/10.1016/j.desal.2014.07.007.

Zulkefli, S., Abdulmalek, E., & Abdul Rahman, M. B. (2017). *Pretreatment of oil palm trunk in deep eutectic solvent and optimization of enzymatic hydrolysis of pretreated oil palm trunk*. *Renewable Energy*, *107*, 36–41. https://doi.org/10.1016/j.renene.2017.01.037.